2020

Old and deer: A study of Neoarchean Peridotites in Michigan's Upper Peninsula

Rachel Merz

Old and deer: A study of Neoarchean Peridotites in Michigan's Upper Peninsula

Abstract

The Deer Lake Peridotite and the Presque Isle Periodotite are two ultramafic formations of Neoarchean age within the Ishpeming Greenstone Belt of Michigan's Upper Peninsula, and are found only fifteen miles apart. The Deer Lake Peridotite was deformed in processes indicative of the broader, regional-scale tectonics of the region, but little study has been done on the mineralogy and extent and style of alteration. This research aims to better classify the mineralogy of the formation, with particular focus on textural variations observed in thin-section, as well as chemical analysis of samples taken from the formation. In addition, this research seeks to correlate the Deer Lake Peridotite's history of alteration, which may have included alteration by Proterozoic events, with that of the Presque Isle Black Rocks, a formation which has had more extensive study done on its tectonic history and alteration. The comparison between alteration styles in the two formations will help draw conclusions about the tectonic history of Michigan's Upper Peninsula.

Degree Type

Open Access Senior Honors Thesis

Department

Geography and Geology

First Advisor

Dr. Christine M. Clark

Second Advisor

Dr. Steven T. LoDuca

Third Advisor

Dr. Rick Sambrook

Subject Categories

Geology

OLD AND DEER: A STUDY OF NEOARCHEAN PERIDOTITES IN MICHIGAN'S UPPER PENINSULA

By

Rachel Merz

A Senior Thesis Submitted to the

Eastern Michigan University

Honors College

in Partial Fulfillment of the Requirements for Graduation

with Honors in Geology

Approved at Ypsilanti, Michigan, on this date March 25, 2020

Supervising Instructor: Dr. Christine M. Clark Date: 4/9/2020

Departmental Honors Advisor: Dr. Steven T. LoDuca Date: 4/8/2020

Department Head: Date: 4-9-2020

Honors Director: Dr. Ann Eisenberg Date: 5/12/2020

Old and Deer:

A Study of Neoarchean Peridotites in Michigan's Upper Peninsula

Abstract: The Deer Lake Peridotite and the Presque Isle Periodotite are two ultramafic formations of Neoarchean age within the Ishpeming Greenstone Belt of Michigan's Upper Peninsula, and are found only fifteen miles apart. The Deer Lake Peridotite was deformed in processes indicative of the broader, regional-scale tectonics of the region, but little study has been done on the mineralogy and extent and style of alteration. This research aims to better classify the mineralogy of the formation, with particular focus on textural variations observed in thin-section, as well as chemical analysis of samples taken from the formation. In addition, this research seeks to correlate the Deer Lake Peridotite's history of alteration, which may have included alteration by Proterozoic events, with that of the Presque Isle Black Rocks, a formation which has had more extensive study done on its tectonic history and alteration. The comparison between alteration styles in the two formations will help draw conclusions about the tectonic history of Michigan's Upper Peninsula.

Acknowledgements:

A heartfelt thanks must be given to my research advisor Dr. Christine Clark without whom this quality of research would not have been possible and, had it commenced nonetheless, would have been much more disappointing.

Thanks to Dr. Katherine Ryker for her field assistance in the form of hauling my samples (more specifically a sample named Cragory) from the field. Thank you to Tina Hill from Bruker for my first batch of XRF tests for free and thank you as well to every rogue geologist at GSA 2018 who helped identify thin-sections at the table in the lobby.

Thank you to the Eastern Michigan University Undergraduate Research Grant and the Michigan Space Grant Consortium for funding this endeavor.

Thanks also to my good friends too numerous to name who, if they've decided to embark on the considerable task of reading a thesis on geology, know who they are. Thank you for constant support and patience.

Thank you to my parents, Joyce and Edward Merz, who never stopped me from keeping rocks under my pillow, and my siblings, Elizabeth Harmsen and Joshua Merz, who each pursue their own endeavors and let me play in the dirt peacefully.

A final thank you to Jon "Monty" Montgomery who, in the 6th grade, told us all we needed to thank him in any published endeavor. I remember.

Table of Contents:

Objectives:

Ultramafic rocks, those that make up the inner layers of the Earth, known as the mantle, are a relative rarity at Earth's surface. Because direct testing cannot be done on rocks within the planet, data about the Earth's mantle must be extrapolated from ultramafic material found at the surface. Several ultramafic units of Neoarchean age are located within Michigan's Upper Peninsula. Of particular interest to this project is the Ishpeming Greenstone Belt.

This project's intent is to compare the alteration of the two sites with the purpose of analyzing the metamorphic and tectonic processes that were occurring in the area in the Archean, particularly concentrating on the alteration across the formations and any history of multiple alteration events. This project also serves to investigate whether or not the two sites share common magma sources, and, if so, why then the two sites contain rocks altered in such dramatically different styles.

Background:

Location

This research focuses on two research sites: the Deer Lake Peridotite and the Presque Isle Peridotite, commonly called the Presque Isle Black Rocks. Both research sites are located in Marquette County, Michigan. Marquette is the largest county in the state, and the largest city in Michigan's Upper Peninsula. Bedrock in the county ranges in age from Neoarchean to Paleoproterozoic (Moorey and Van Schmus, 1988). The Marquette area also contains a third notable peridotite body, the Yellowdog Peridotite, but this third body was not included in this project. These ultramafic rocks in Michigan's Upper Peninsula constitute some of the oldest rocks in Michigan (Bornhorst and Johnson, 1993).

The two research sites are located in the southern half of the Ishpeming Greenstone Belt, which is dominantly a greenstone-granite terrane. These greenstones represent the southernmost Archean formations in the Superior province, the craton that forms the core of the Canadian Shield, north of Lake Superior and extending north to Hudson Bay. The Ishpeming Greenstone

Belt is intruded by several bodies, including two peridotite bodies. The intruding bodies are Archean in age, likely dating 2700Ma or earlier (Bornhorst and Johnson, 1993).

Peridotite

Peridotite is a rock composed of between 40 and 100 percent olivine and constituted otherwise by pyroxenes and minimal plagioclase. These are minerals that contain a high percentage of iron and magnesium, elements that preferentially enter crystalline structures and are therefore more concentrated in the earliest minerals that solidify from melt. While the classification of peridotite is given to any rock with an olivine component of greater than 40%, several sub-classifications of peridotite exist, including dunite (90% or more olivine), harzburgite (40-90% olivine, and with a pyroxene fraction of at least 95% orthopyroxene), wehrlite (40-90% olivine, but with a pyroxene fraction of at least 95% clinopyroxene), and lherzolite, the most common variety (40-90% olivine, and a pyroxene fraction ranging between 95% clinopyroxene and 95% orthopyroxene) (Woolley et al., 1996).

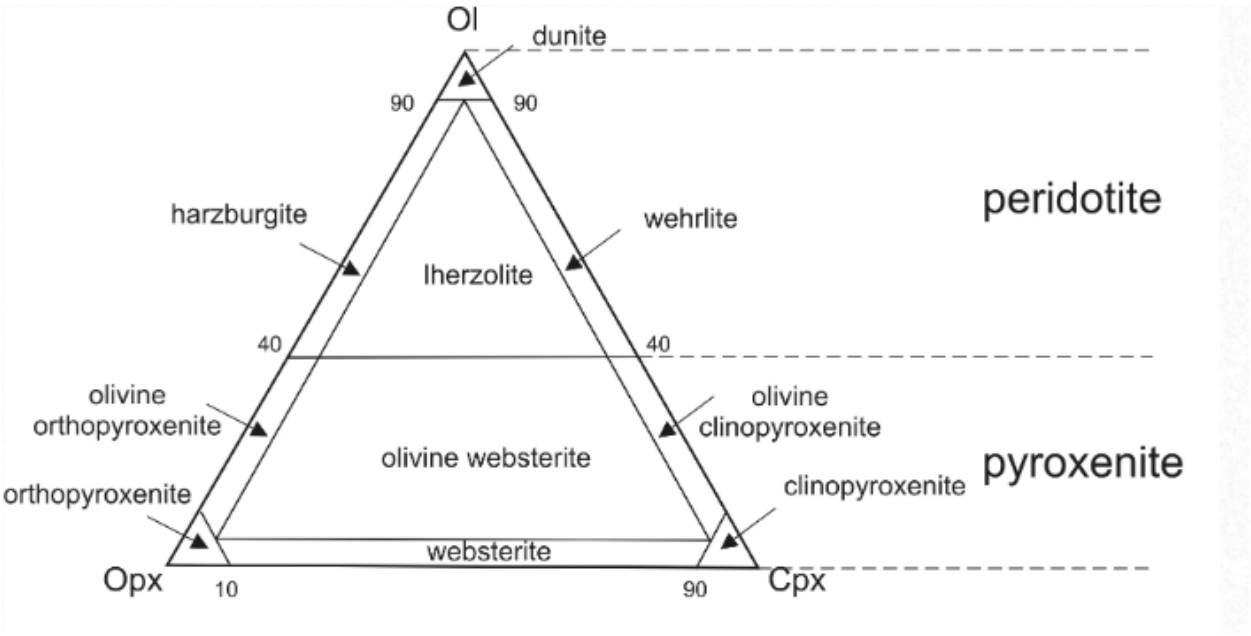

Figure 1: Ternary diagram for mafic plutonic igneous rocks. (Adapted from Woolley et al., 1996)

Ultramafic rocks are dark in color which, for these two locations, means the white veins of alteration stand out clearly. In the case of the Presque Isle Black Rocks, the veins are made of carbonates, though which carbonate is more difficult to say. Calcite and dolomite are the two main suspects, as supported by XRF data. The veins in the Deer Lake Peridotite are composed of far more fibrous material, and have a composition of sulfur, nickel, and copper and, to a lesser extent, carbonate and silicate material.

The Deer Lake Peridotite is a mafic to ultramafic sill of Neoarchean age (Bornhorst and Johnson, 1993) and is composed largely of serpentine-group minerals, a subgroup consisting of a variety of minerals. The three most common minerals within this group are the chemically identical polymorphs antigorite, lizardite, and chrysotile. Serpentine-group minerals occur as a result of the alteration of olivine under intense pressure and heat, in the presence of water. Lizardite and chrysotile are low-temperature polymorphs, while antigorite is the higher temperature polymorph, typically not forming until temperatures reach upwards of 250℃ (Woolley et al., 1996).

Tectonics

The Great Lakes Tectonic Zone (GLTZ) is a major Precambrian crustal feature that extends from Minnesota into Ontario, Canada, and separates the regions Archean gneissic terrane in the south from the younger Archean greenstone-granite terrane in the north. The zone was marked by compressional forces during the Algoman Orogeny (roughly 2.7 Ga), followed by extensive pull-apart tectonics (2.45-2.1 Ga), massive compression during the Penokean Orogeny (1.9 Ga-1.85 Ga), then a second extensional period in the Middle Proterozoic (1.6 Ga), with a minor compressional reactivation within the past 500 Ma (Sims et al., 1980; Sims and Day, 1995).

Geologic mapping in Marquette has revealed the structure of the GLTZ along a 10 km length of an active dextral strike-slip zone south of the city, directly under the Marquette anticline, and it is proposed by Sims and Day (1995) that the consistent kinematics along this exposed length are applicable across the whole of the GLTZ. The northwest-striking zone of the GLTZ through 2 km of metamorphic rock resulted in shear boundaries marked by mylonite exposed at the Presque Isle Peridotite outcrop. Deformation of the Marquette Range Supergroup

sediments occurred following the compressive deformation resulting from the reactivation of the GLTZ during the Penokean Orogeny (Sims and Day, 1995).

Methodology:

Samples were collected from the field both in 2018 and 2019. Samples collected in 2018 were collected April 30, 2018 and May 2, 2018. Additional samples were collected on May 1, 2019 from both locations. Trend and plunge data for the Presque Isle location were also taken.

Locations

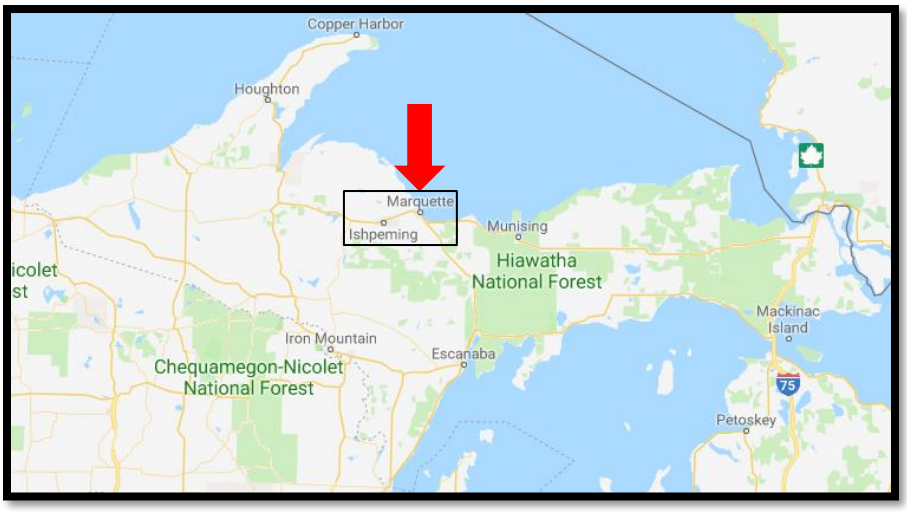

Figure 2: Map of Michigan's Upper Peninsula showing the location of the research sites. (Google. (n.d.) [Map of Michigan's Upper Peninsula]. Retrieved February, 2020)

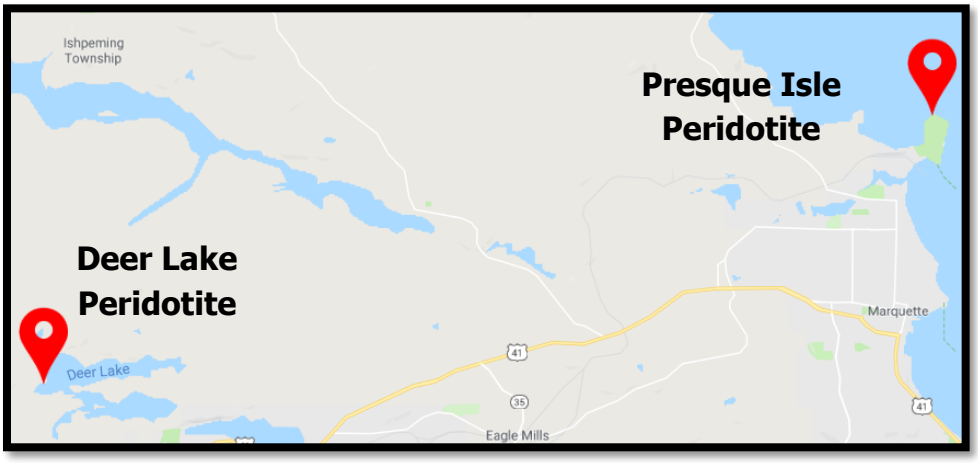

Figure 3: Map of the Marquette, Michigan area showing the locations of the two research sites. (Google. (n.d.) [Map of Two Study Locations]. Retrieved February, 2020)

The Presque Isle Black rocks constitute a peninsula jutting into Lake Superior north of Marquette. Samples were collected from the northern end of this peninsula. The Deer Lake Peridotite is exposed along the western shore of Deer Lake in Ishpeming, as well as in multiple outcrops dotting the lake itself. For this project, Deer Lake Peridotite samples were taken exclusively from the County Rd 573 exposure.

Field Observations

Presque Isle:

The Presque Isle Black Rocks are exposed along the shore of Lake Superior. Waves frequently break over them, and several coves have been eroded into the rock face, resulting both in highly weathered, easily broken rock and steep cliff faces ending abruptly in the lake (Figure 4-6). The highly weathered nature of these rocks makes it vital to create a fresh surface for observation (Figures 7 and 8). Immediately to the west of the main study area the same rocks, marked by their characteristic white veins, have had the iron within them oxidized such that they no longer appear black, and rather are a light brown in color. The rocks found at this location are slightly, but noticeably, magnetic.

The dark surface of the rock is cross-cut by vibrant white veins of alteration, which are not magnetic. Several episodes of tectonic activity have resulted in the Black Rocks being highly fractured, with the dominant trend of fractures being to toward the south and west. Northwest-trending mylonite, vivid green and yellow in color, is found on many surfaces throughout the exposure and can be easily broken off with a rock hammer. Within rock fractures at this location are large, easy to see white veins of carbonate material that react violently with HCl.

Figure 4: West end of the Black Rocks exposure Rocks exposed in the left most portion of this photo have been weathered to brown. The white carbonate veins stand out in both appearance and relief.

Figure 5: Middle portion of the Black Rocks exposure The Black Rocks are a large and mostly flat exposure of ultramafic rock. It has been highly fractured across its exposure.

Figure 6: East end of the Black Rocks exposure The waves battering the Black Rocks have left steep cliffs.

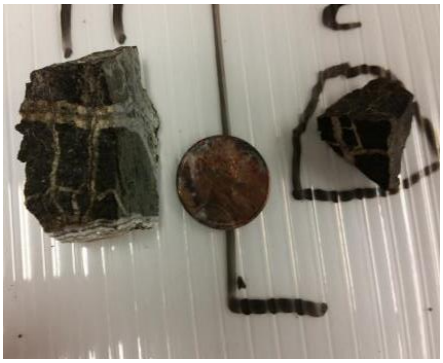

Figure 7: Presque Isle Peridotite sample showing white alteration veins. Penny for scale.

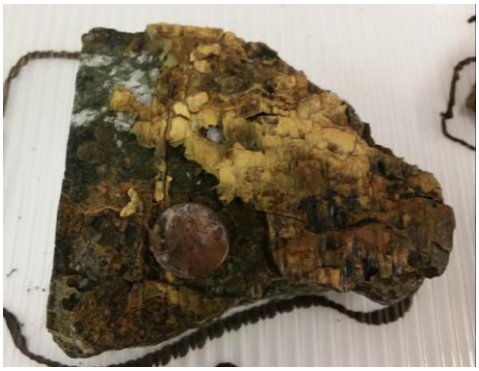

Figure 8: Presque Isle Peridotite sample with mylonite surface and scattered carbonate crystals

Deer Lake Peridotite:

The Deer Lake Peridotite is seen in very clear exposures along County Rd. 573, along the shores of Deer Lake (Figure 9). Several other rocky islands dot the lake with outcrops of the peridotite. Being directly on the shore of the inland lake, portions of the outcrop face have been oxidized to reddish brown. The water level observed in 2019 was significantly higher than that observed in 2018.

The alteration to fibrous chrysotile at the Deer Lake location has resulted in many sections of the rock face appearing nearly like wood, which is easily pulled apart. While this exposure has also been affected by tectonic processes, the fault lines resulting from this are much less pronounced than is the case with the Black Rocks. The dominant direction of faulting is also to the southeast, rather than the southwest. The Deer Lake Peridotite has a slight magnetic pull, despite many portions not showing visible magnetite. Opaque minerals, likely magnetite, are visible, however, in thin-section.

Figure 9: Image showing the location from with Deer Lake Peridotite samples were collected

Data:

Several styles and sources of data were used for this project. Of the many hand-samples collected, a select number were made into thin-sections. Several hand-samples, cut down to a manageable size, were also evaluated for XRF imaging using a Bruker M4 Tornado. For three samples (43018.1, 43018.1b, and 50218.1b), bulk-composition data were collected at the time of XRF data. These thin-sections are approximately 30 μm (0.03 mm) thin and 26 mm by 46 mm, sealed with clear epoxy. All thin-sections and XRF data is displayed in Appendix 1 and 2, respectively.

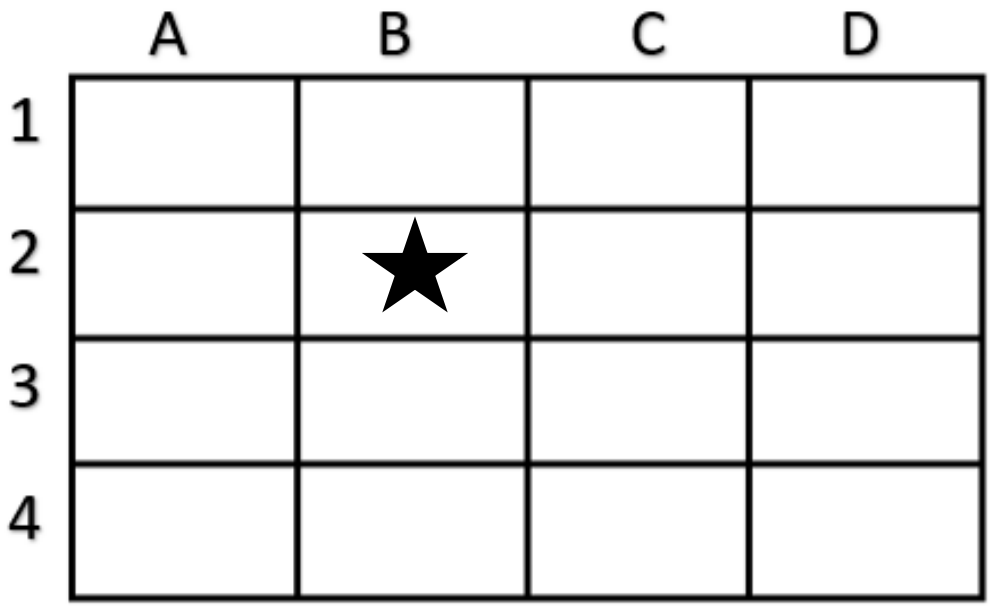

Figure 20: Thin section reference guide. The above chart shows how locations on slides will be referred to in the following discussion. For example, if a particular image cites section 2B, the reader may assume the marked segment contains that structure.

Sample 43018.1B:

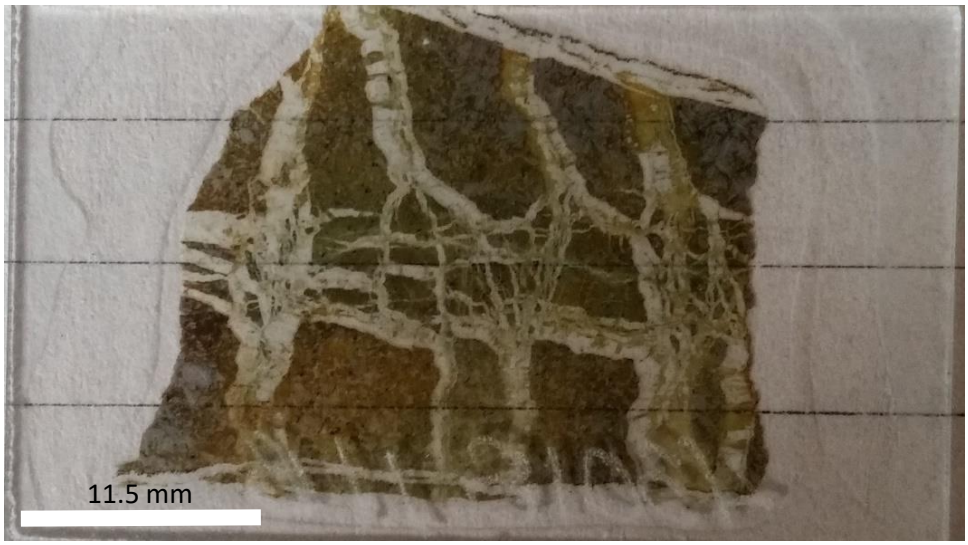

Figure 11: Sample 430181.1B thin-section

This sample is from the Presque Isle Peridotite. It shows a black matrix divided by bands of carbonation. Generations of carbonization are visible within the veins (Figure 11). The XRF imaging on this sample makes it very evident that Ca has mobilized into hydrothermal veins, while Mg, Fe, and Si have stayed in the bulk rock. Section i in Appendix 2 contains further XRF data for this sample.

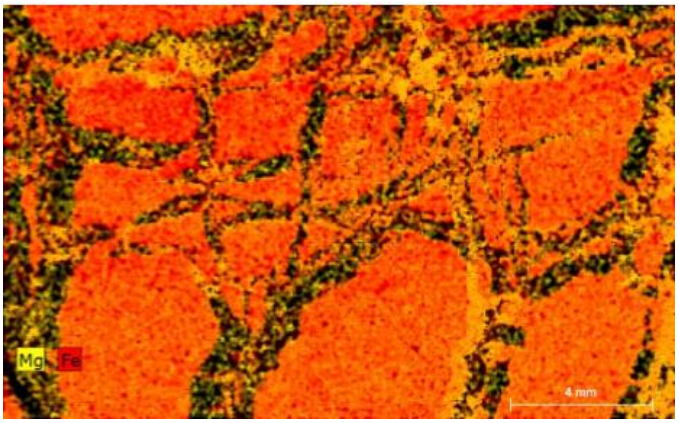

Figure 12: XRF image showing the distribution of Mg in yellow and Fe in red in sample 43018.1B

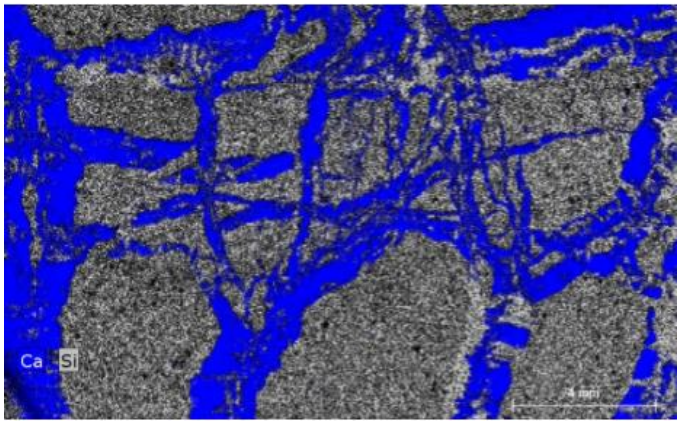

Scan 13: XRF image showing the distribution of Ca in blue and Si in grey in sample 43018.1B

Sample 43018.1:

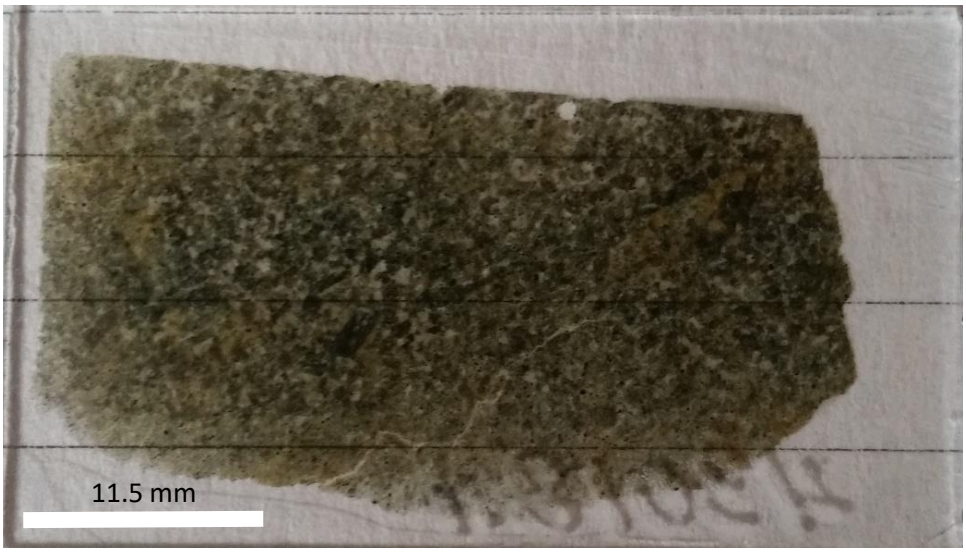

Figure 14: Sample 43018.1 thin-section

This sample was collected from the Presque Isle Peridotite. Both with and without microscopic magnification, it is easy to see the largely uniform texture of this thin-section. Though the minerals are randomly oriented across the face of the sample, with the only interruption of the mass being the light carbonate veins seen extending from B4 to C3 (Figure 14).

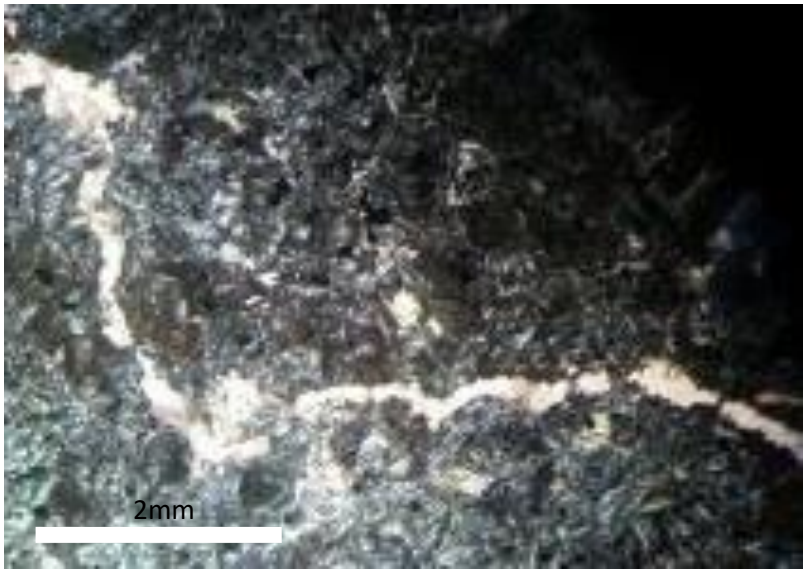

Figure 15: Magnified view of carbonate vein in sample 43018.1 in XPL.

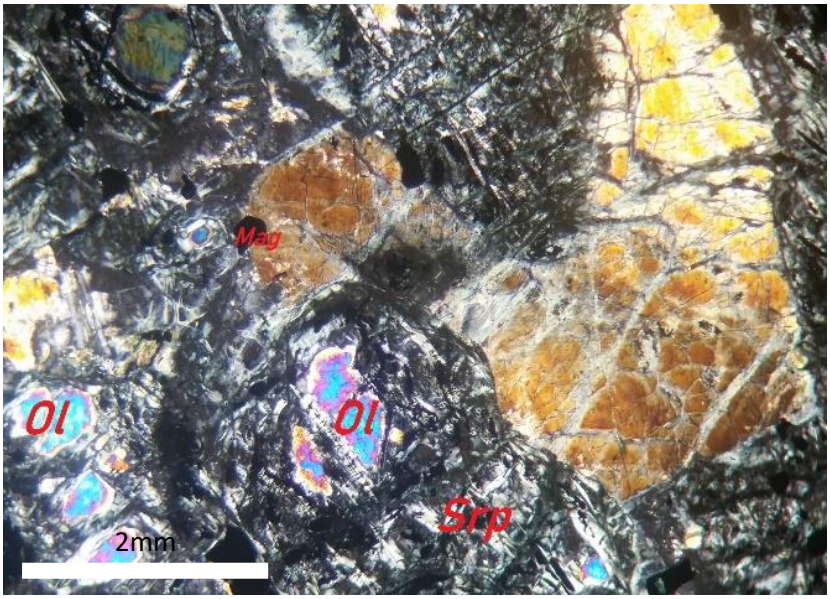

Figure 16: Magnified view of minerals visible in sample 43018.1. Ol is olivine, Srp is serpentine mineral, Mag is magnetite (XPL, 100x mag)

It is likely that the veins cutting through the large crystal on the right side of the slide are composed of a serpentine polymorph, though it is difficult to differentiate species of serpentine apart from one another in thin-section.

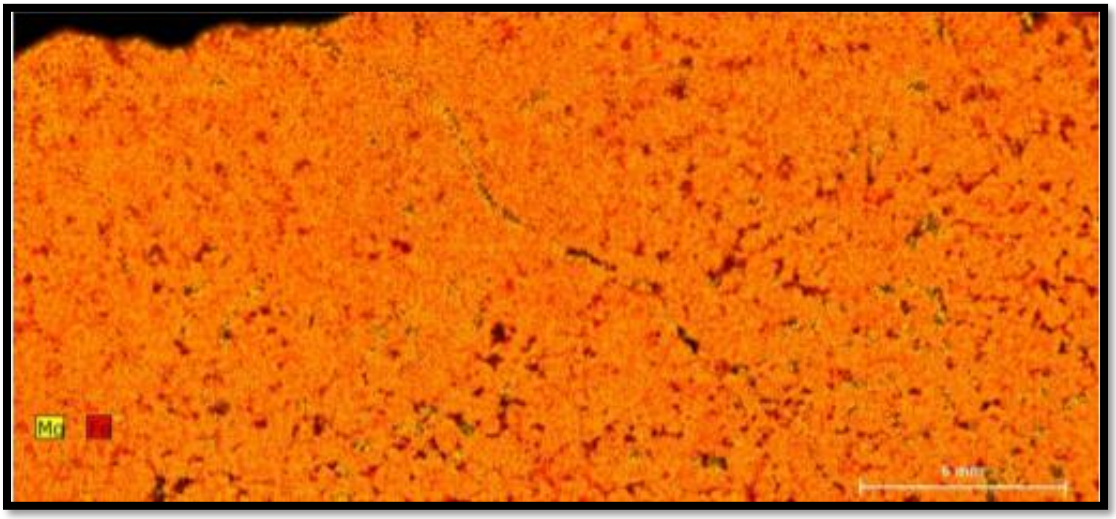

Figure 17: XRF image of sample 43018.1 showing the distribution of Mg in yellow and Fe in red.

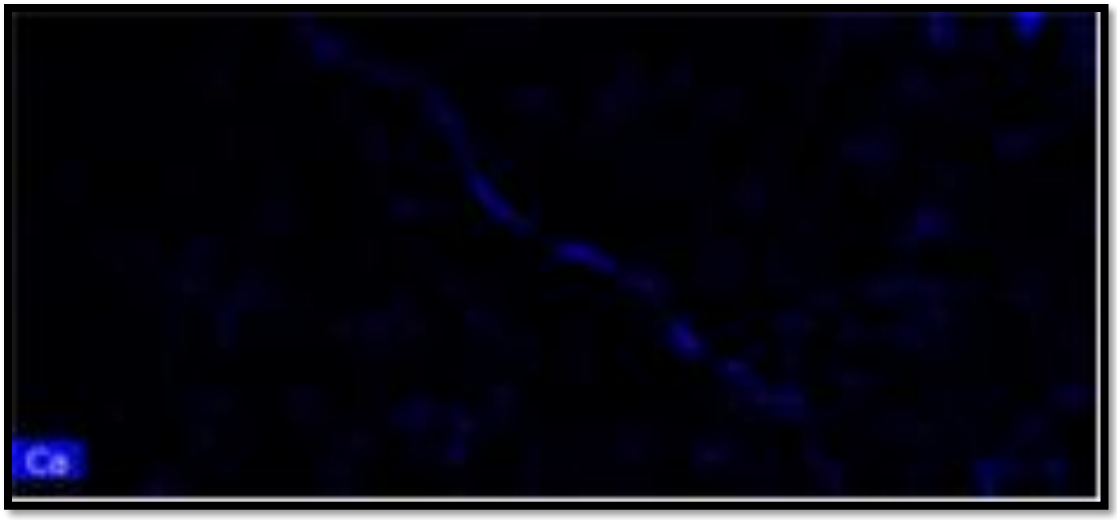

Figure 18: XRF image of sample 43018.1 showing the distribution of Ca in blue.

The XRF data shows that Fe and Mg remain in the mass of the rock, while the light veins are composed largely of Ca, consistent with previous research (Bornhorst and Johnson, 1993). Section ii in Appendix 2 contains further XRF data for this sample.

Sample 50218.10:

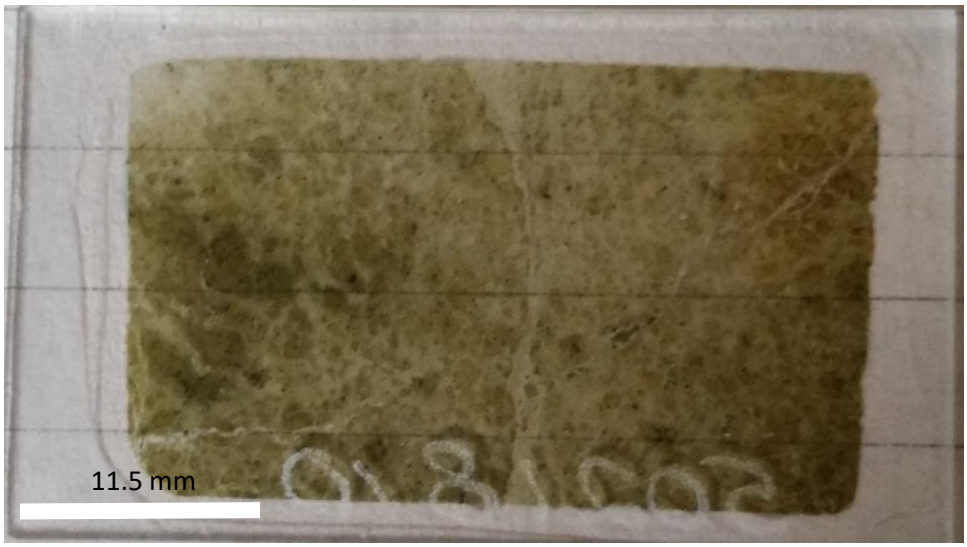

Figure 19: Sample 50218.10 thin-section

This sample was collected from the Deer Lake Peridotite. Sample 50218.10 shows the typical generations of serpentinization, with regions of antigorite, lizardite, and chrysotile. Small magnetite crystals are unevenly scattered throughout. The material showing as brown in the above image is augite. In thin-section an undulatory extinction is visible in primary olivines altered to chrysotile.

Sample 50218.1B:

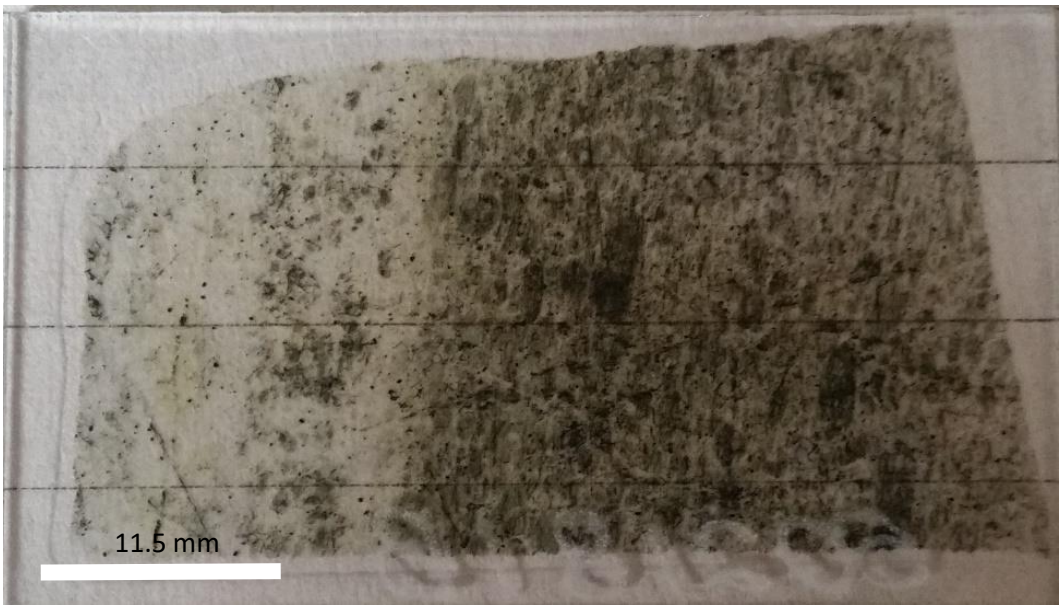

Figure 20: Sample 50218.1B thin-section

This sample was collected from the Deer Lake Peridotite. In this slide it is seen that the pyroxene is a more recent alteration within the body. The large, oblong black speck between C2 and B2 (Figure 19) is an altered pyroxene crystal.

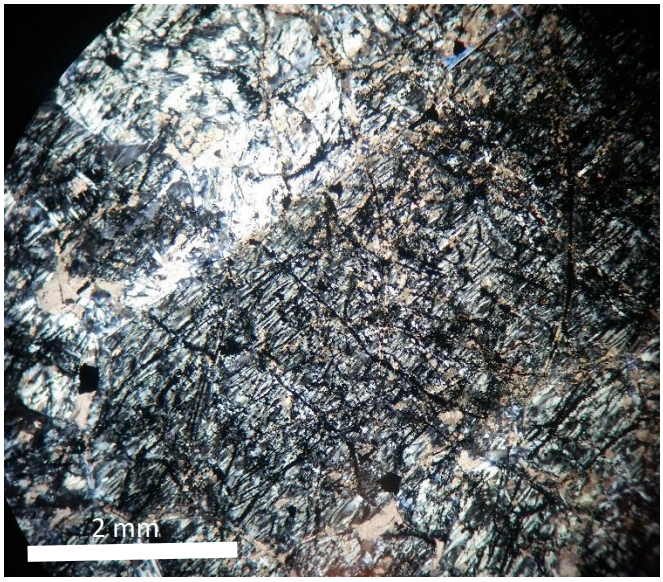

Figure 21: Magnified view of sample 50218.1B showing the magnified pyroxene crystal in XPL.

The above is a magnified view of this alteration of a pyroxene crystal, which has occurred more recently than the alteration of the surrounding mass, resulting in it retaining a crystalline shape amidst otherwise optically unidentifiable material.

XRF imaging shows a generation of serpentinization across the face of the thin-section sample, from the outside of the hand-sample to the more inward of the rock body. This sample in particular is from a very large piece of the Deer Lake Peridotite, and one that shows a vivid green rind around the exterior of the rock body (Figure 22).

Figure 22: Sample 50218.1B in hand-sample. Penny for scale. Hand-sample is roughly 45 cm to a side.

XRF imaging shows the green rind has higher amounts of Mg and Ni, with Fe becoming more dominant toward the center of the rock (Figure 79 and Figure 80, in Section iii, Appendix 2). The white veins visible in hand-sample contain Al, Cu, Ni, S, and Si (Section iii, Appendix 2).

Sample 50218.16:

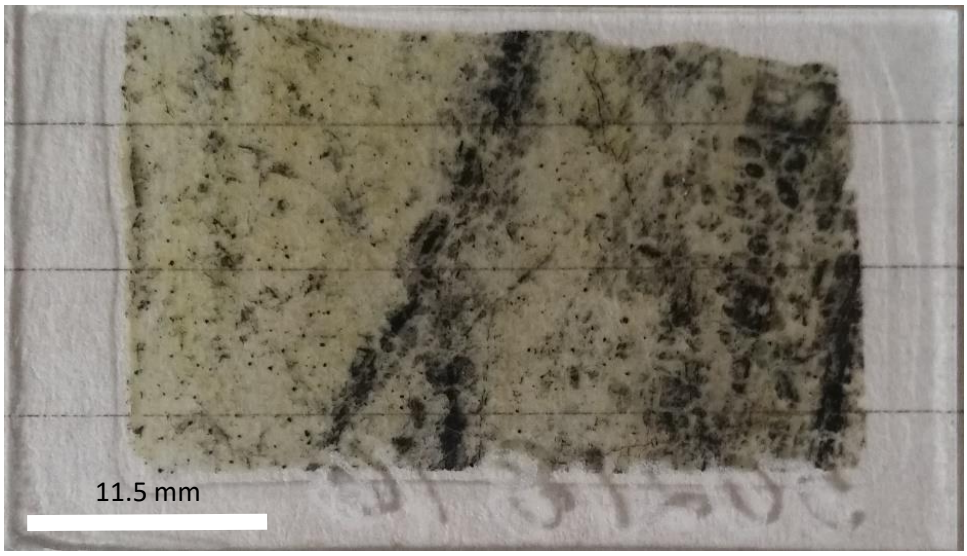

Figure 23: Sample 50218.16 thin-section

Sample 50218.16 shows a scattered array of optically unidentifiable microlites, as is the case with many of the sample from the Deer Lake Peridotite. Several large, opaque magnetites are visible across the thin-section, both magnified and to the naked eye.

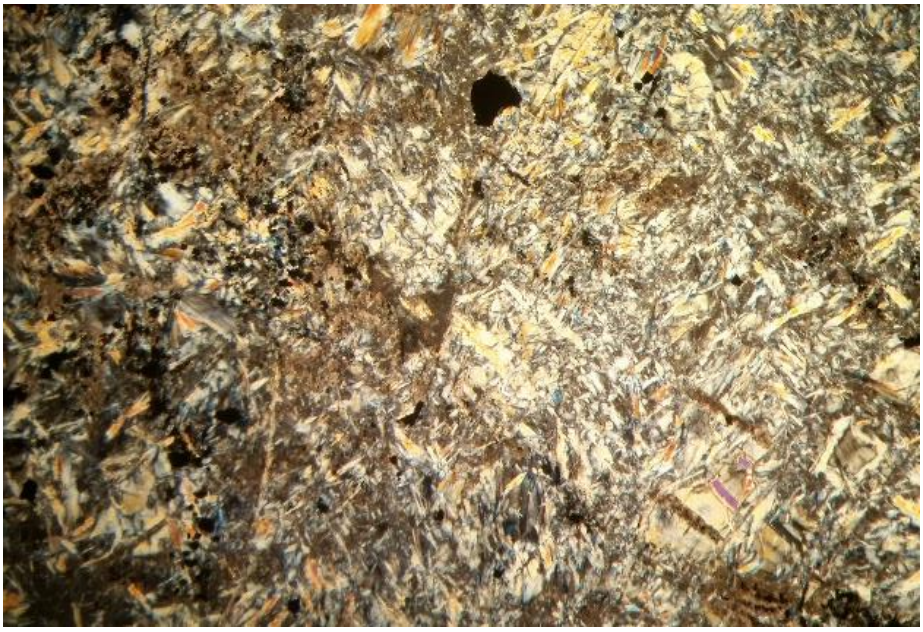

Figure 24: Magnified view of sample 50218.16, the majority of these minerals are too small to be optically identified (XPL, 100x).

Sample 50218.22:

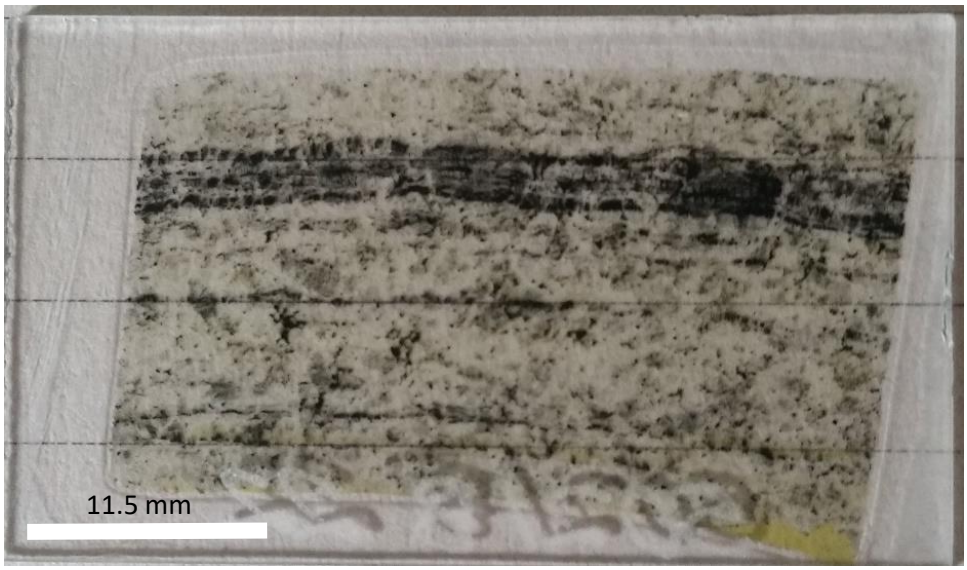

Figure 25: Sample 50218.22 thin-section

In thin-section, a band of dark material is immediately evident in this sample, however a picture of the original hand-sample reveals a less obvious alteration vein. This vein runs form the upper right of the sample to the lower center, and a secondary set of veins meet in a V in the lower left quadrant. XRF data shows that these veins reveal they are composed of Ca and Ti, and to a lesser extent, Cu (Figure 27, Figure 28, Figure 29). Section vi in Appendix 2 contains further XRF data for this sample.

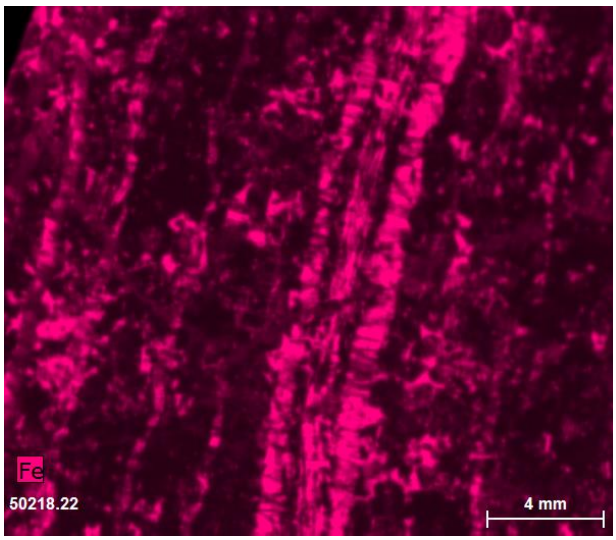

Figure 26: XRF image showing dark bands in thin-section 50218.22 are primarily Fe

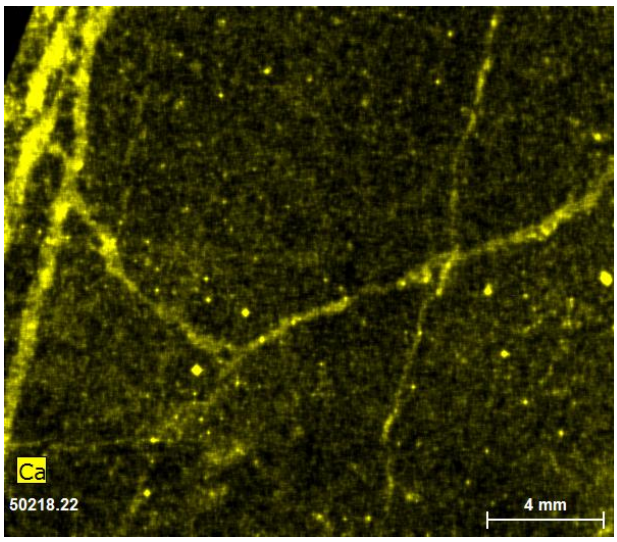

Figure 27: XRF image showing alteration bands in sample 50218.22 contain Ca

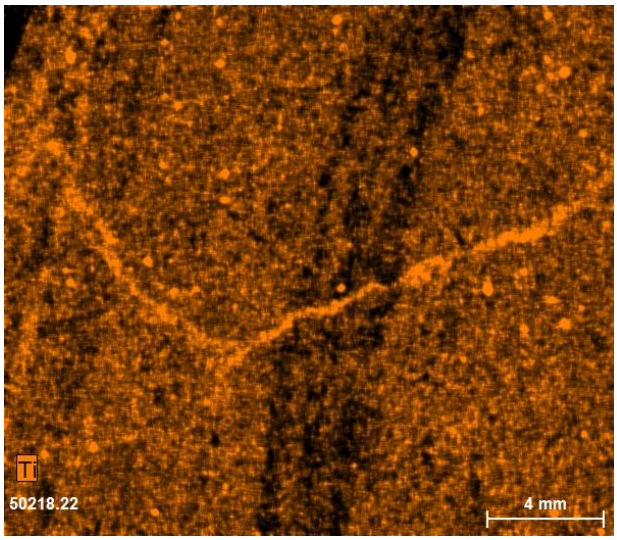

Figure 28: XRF image showing alteration bands in sample 50218.22 contain Ti

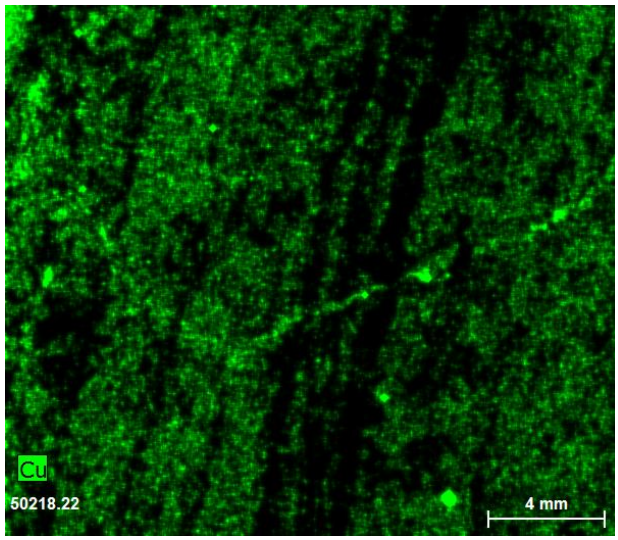

Figure 29: XRF image showing alteration bands in sample 5021.22 contain Cu

Sample 502181.4:

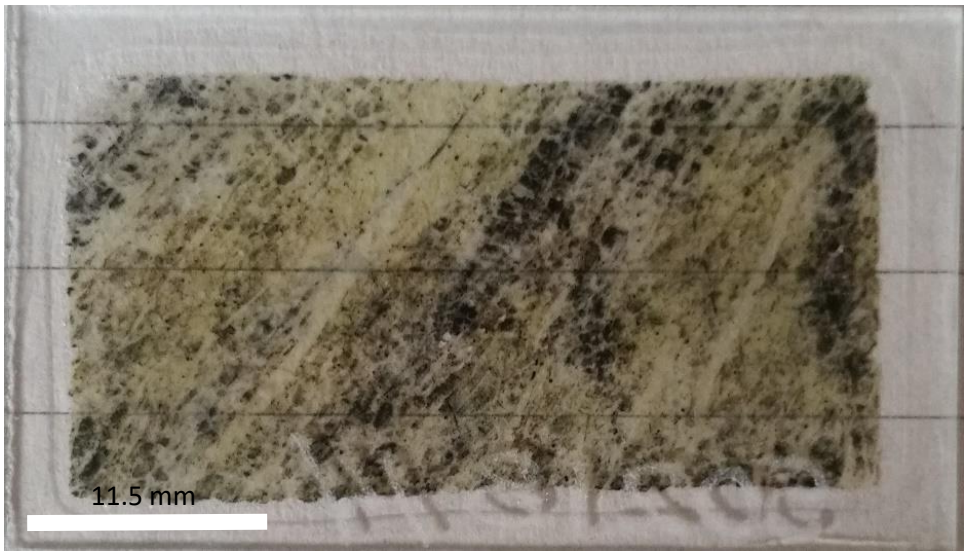

Figure 30: Sample 50218.14 thin-section

This sample was collected from the Deer Lake Peridotite. In hand-sample, sample 502181.4 is highly fibrous, with veins of alteration running diagonally across its surface. Section vii in Appendix 2 contains further XRF data for this sample.

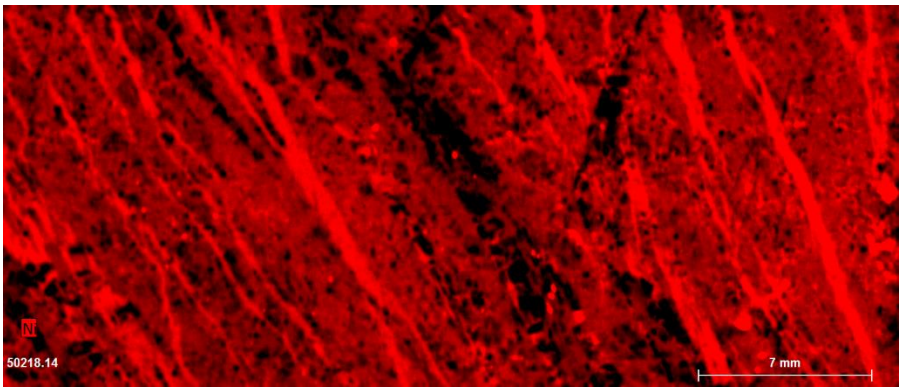

Figure 31: XRF image of sample 50218.14 showing the fibrous alteration of the sample contains Ni

Sample 50218.1C:

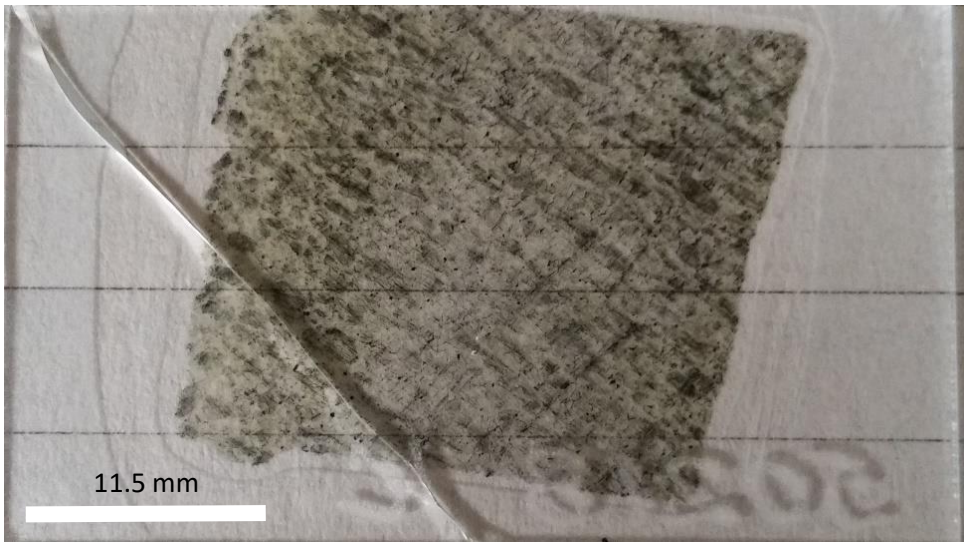

Figure 32: Thin-section of sample 50218.1C

This sample, collected from the Deer Lake Peridotite, has a very uniform arrangement of minerals, and a strong orientation for light minerals. Light streaks seen in thin-section above are bands of chrysotile asbestos. A few magnetites are present but the vast majority of alteration is too small to be optically identifiable, although edges of what were once individual olivine crystals are still visible.

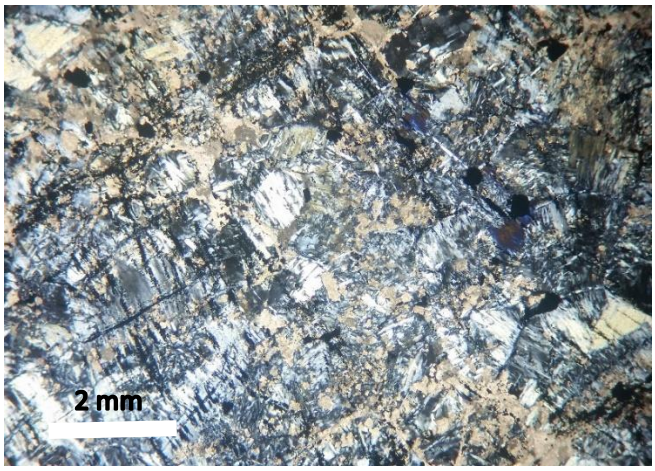

Figure 33: Magnified thin-section image of sample 50218.1C showing the scattered and optically unidentifiable mineral makeup of the sample XPL.

Figure 33 shows a magnified view of the slide revealing that, much of it is too small and altered to be optically identified, but small magnetites can be seen along the upper edge of the image.

Sample 50218.3A:

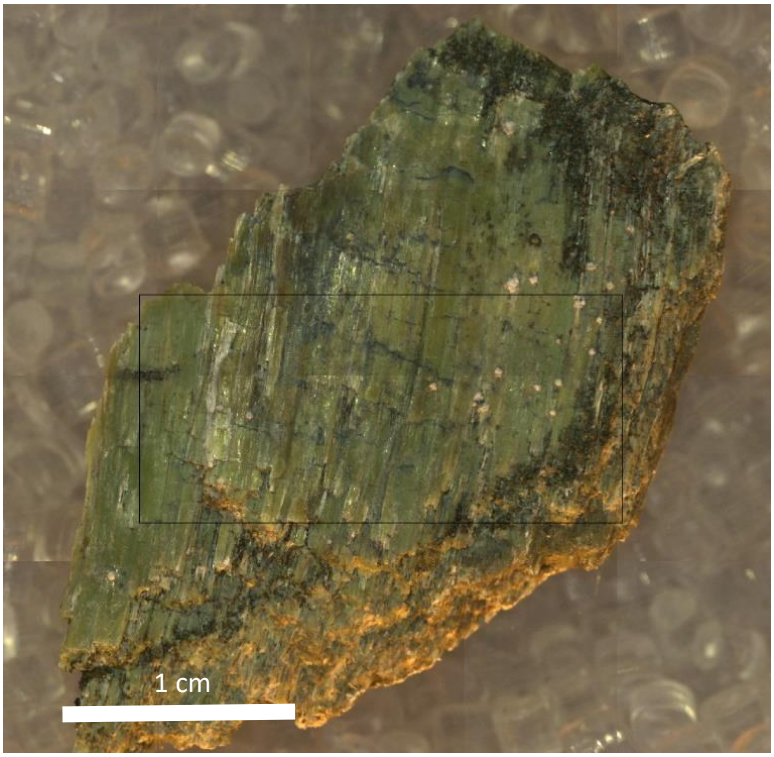

Figure 34: Hand-sample image of sample 50218.3A

While no slides were made of this sample of the Deer Lake Peridotite, this vibrantly green, highly fibrous chip of rock was sent for XRF testing.

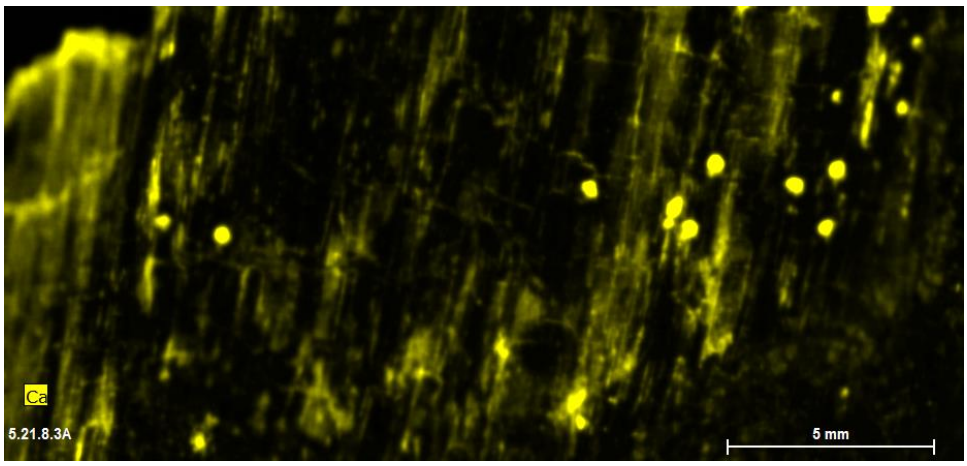

Figure 35: XRF image of sample 50218.3A showing Ca distribution

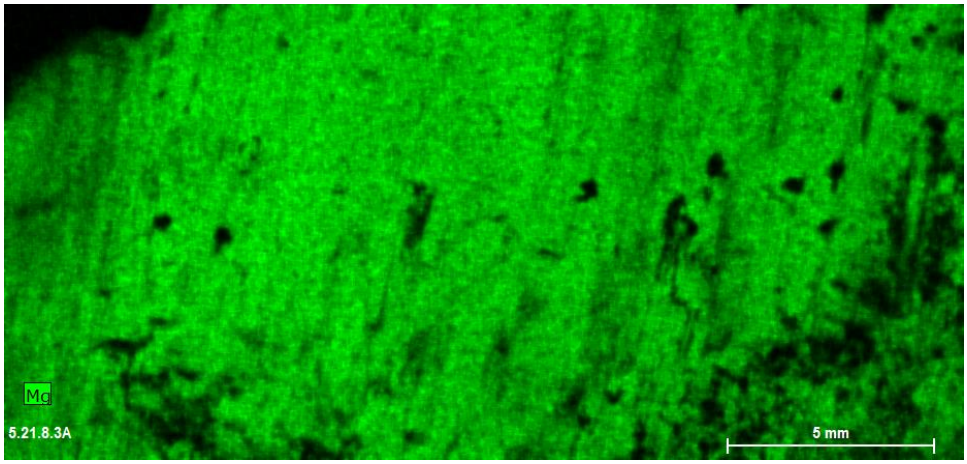

Figure 36: XRF image of sample 50218.3A showing Mg distribution

The XRF scans show the Ca and Mg are directly opposed; that is to say where there is magnesium there is no calcium. This is most evident in the small line of specks in the right portion of the section. Section v in Appendix 2 shows further XRF data for this sample.

Sample DL5119.1:

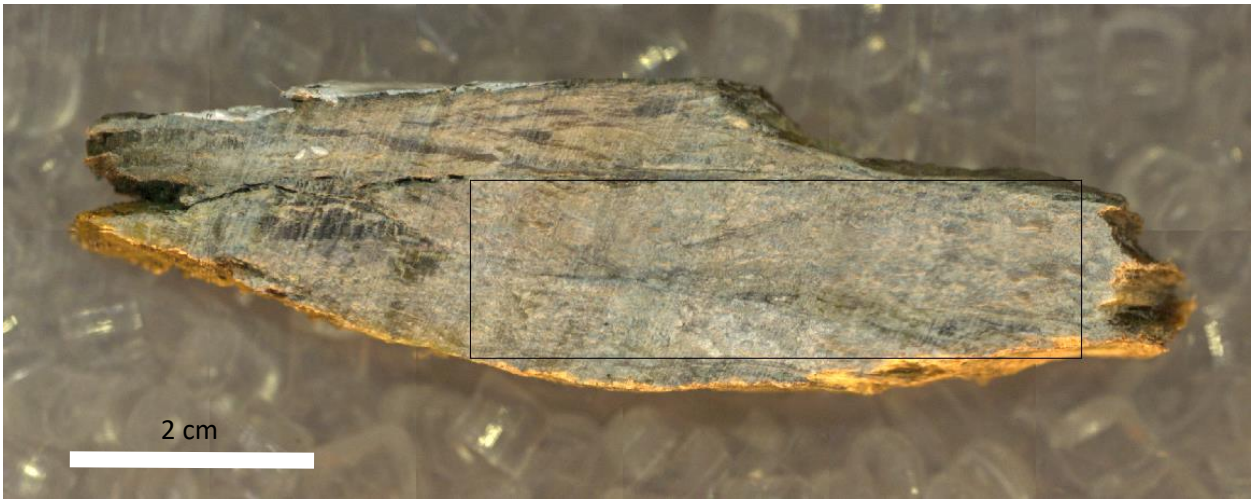

Figure 37: Hand-sample of sample DL5119.1 showing layered fibrous alteration

While no thin-sections were made of this sample of the Deer Lake Peridotite, this rock chip shows multiple layers of fibrous alteration indicative of the habit of the rest of the rock body. Sections of the rock body resembling this one have been so drastically and fibrously alerted that they resemble tree bark.

Figure 38: Hand-sample of sample DL5119.1 showing fibrous alteration. Penny for scale.

Results:

The results of this research helped to confirm previous, albeit limited, research on the area. Differences in alteration styles between the two locations could very well be the result of access to water to hydrate the alteration process. Unfortunately, as can be seen from many of the slide images, much of the two rock bodies is optically unidentifiable due to the extensive alteration that has occurred within the two bodies. The extent of the alteration of the two bodies suggests a prolonged period of alteration, or possibly multiple episodes of alteration.

XRF data of samples taken from the Deer Lake location show multiple instances of alteration bands containing Cu, Ca, S, and Ni. This shows that the alteration processes acting on the Deer Lake Peridotite resulted in Cu, Ca, S, and Ni mobilizing into veins, versus the Ca mobilizing in the case of the Presque Isle Peridotite. This mobilization into veins could not have occurred in a dry environment, and a low pH instigates Ca to move into solution veins. This suggests that the water present for the alteration of the Presque Isle Peridotite was more acidic than that involved in the alteration of the Deer Lake Peridotite.

Conclusions:

Both the Deer Lake Peridotite and the Presque Isle Peridotite are ultramafic bodies, and their close proximity to each other, coupled with the relative rarity of ultramafic rocks, suggests a common source of their magmas, as well as for other ultramafic bodies within the Ishpeming Greenstone Belt. However, primary olivine is far more prevalent within the Presque Isle Peridotite, and very little serpentine is observed as compared to that of the Deer Lake Peridotite, which has far less primary olivine, and is instead highly altered to serpentine, most notably chrysotile.

Differences in these rock bodies can be largely attributed to differences in secondary alternation rather than primary source. While this cannot be definitively proven within the scope of these research project, no evidence to the contrary was found.

That serpentine is found largely in the form of chrysotile within the Deer Lake Peridotite body suggests that the alteration of this body occurred over a longer period of time than that of the Presque Isle Peridotite. The greater extent of alteration as well as the lack of primary olivine further indicates a longer period of alteration. The Presque Isle Peridotite likely experience less

prolonged alteration, as the presence of primary olivine and alteration in veins and around the outside of larger crystals suggests.

While the extent of this research was limited by the complicated nature of the two formations' complicated mineralogy, it has helped to establish a base of information about these bodies that otherwise have had limited study completed on them.

References:

Bornhorst, T., and R. Johnson, 1993. "Geology of Volcanic Rocks in the South Half of the Ishpeming Greenstone Belt, Michigan." *US Geological Survey Bulletin*, doi:10.3133/b1904p.

Morey, G.B., and W.R. Van Schmus, 1988. "Correlation of Precambrian Rocks of the Lake Superior Region, United StatesG.B." *US Geological Survey Professional Paper*.

"Natural Features and Resources." 2008, *Marquette Comprehensive Plan*.

Sims, P. K., K.D. Card, G.B. Morey, Z.E. Peterman, 1980. "The Great Lakes Tectonic Zone — A Major Crustal Structure in Central North America." *Geological Society of America Bulletin,* vol. 91, no. 12, p. 690., doi:10.1130/0016-7606(1980)912.0.co;2.

Sims, P. K., and W. C. Day, 1995. "New Data on Vergence of the Late Archean Great Lakes Tectonic Zone." *Proceedings of the International Conferences on Basement Tectonics*, pp. 409–412., doi:10.1007/978-94-017-0831-9_37.

Woolley, A.R, S.C. Bergman, A.D. Edgar, M.J. LeBas, R.H .Mitchell, N.M.S. Rock, B.H. Scott Smith, 1996. "Classification of Lamprophyres, Lamproites, Kimberlites, and the Kalsilitic, Melilitic, and Leucitic Rocks." *The Canadian Mineralogist*, vol. 34.

Yin, A., 2004. "Gneiss Domes and Gneiss Dome Systems." *Gneiss Domes in Orogeny*, doi:10.1130/0-8137-2380-9.1.

Appendix 1: Thin-Sections

These thin-sections are approximately 30 µm (0.03 mm) thin, 26 mm wide by 46 mm long, and sealed with clear epoxy.

Presque Isle Peridotite Thin Sections:

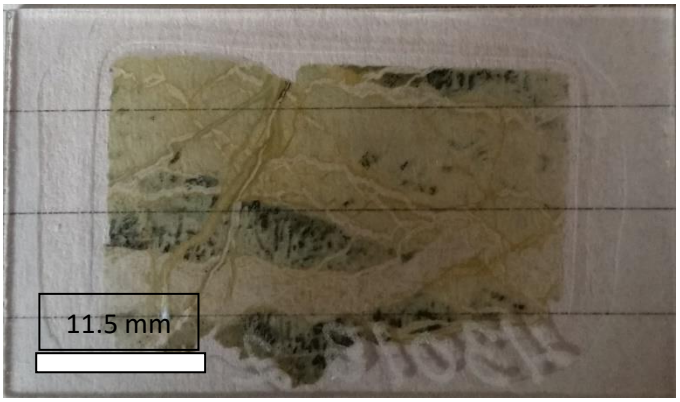

Figure 39: Sample 43018.2 thin-section

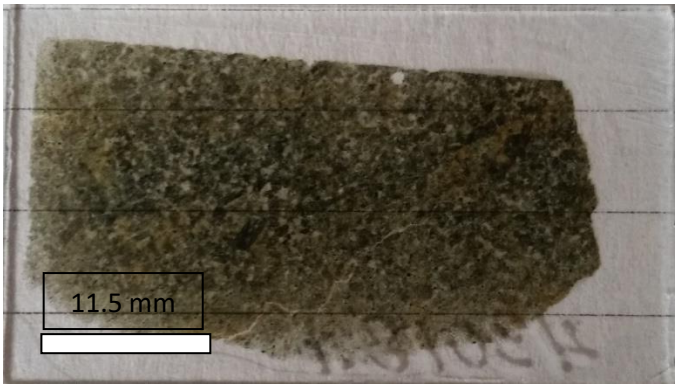

Figure 14 : Sample 43018.1 thin-section

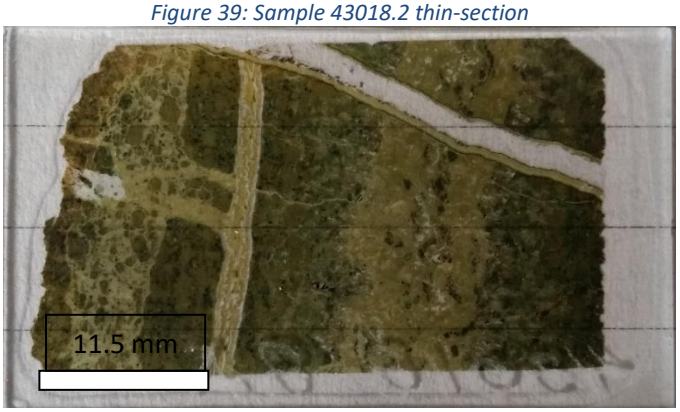

Figure 40 : Sample 43018.8A thin-section

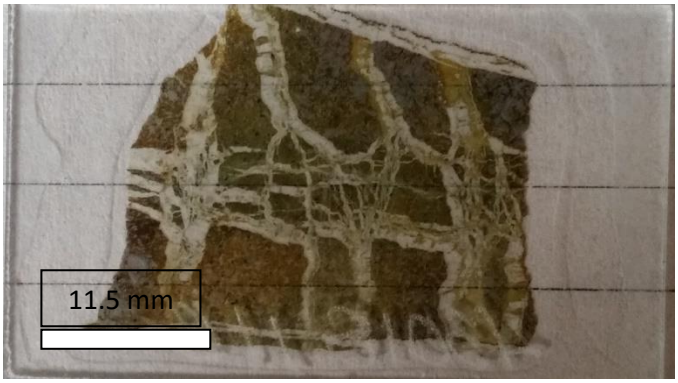

Figure 11: Sample 430181.1B thin-section

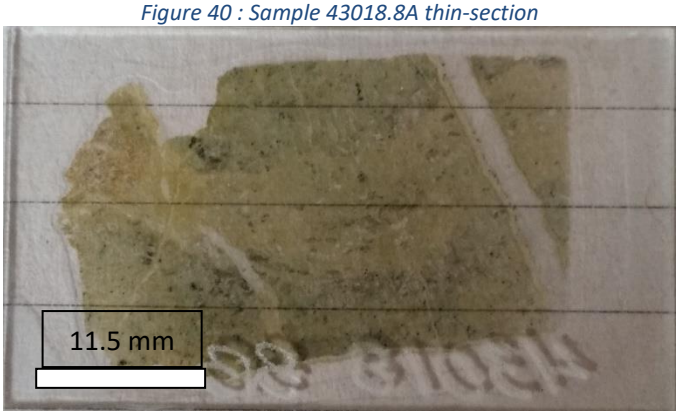

Figure 41 : Sample 43018.8B thin-section

Deer Lake Peridotite Thin-Sections:

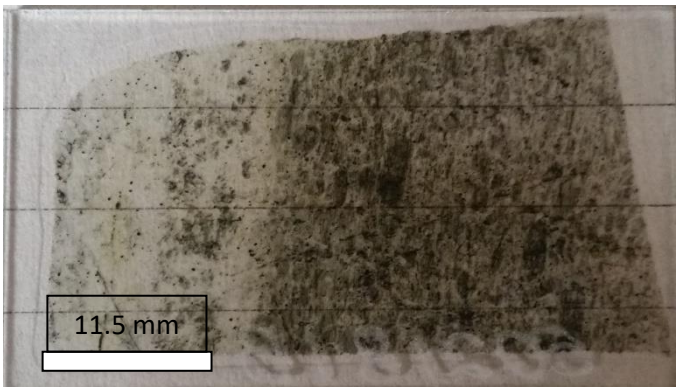

Figure 20: Sample 50218.1B thin-section

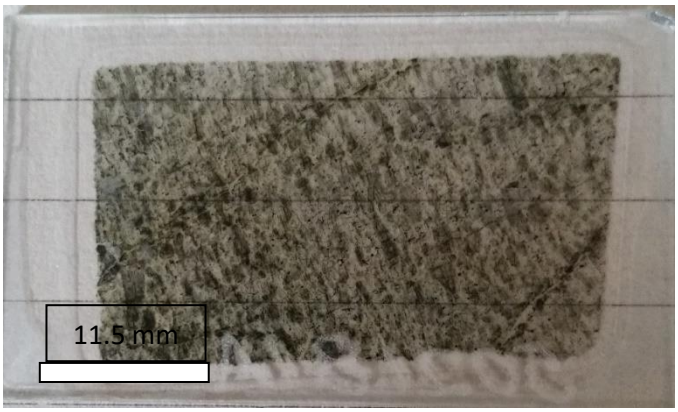

Figure 42: Sample 50218.1A thin-section

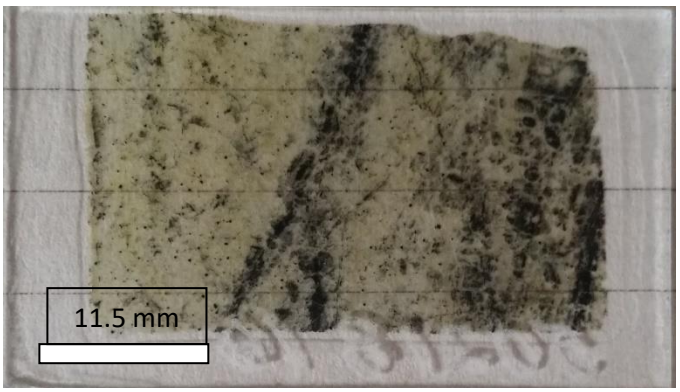

Figure 23: Sample 50218.16 thin-section

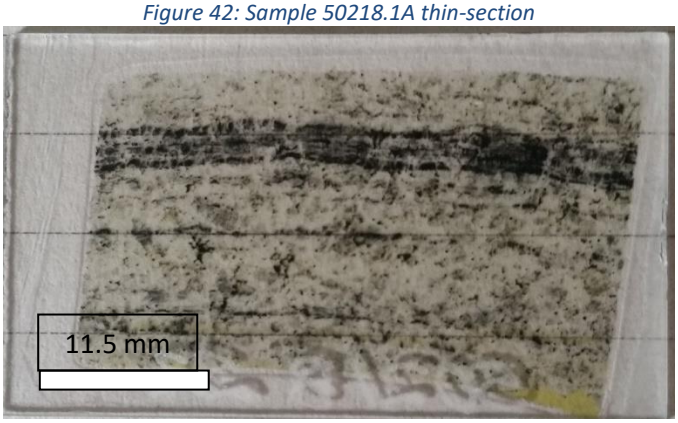

Figure 25: Sample 50218.22 thin-section

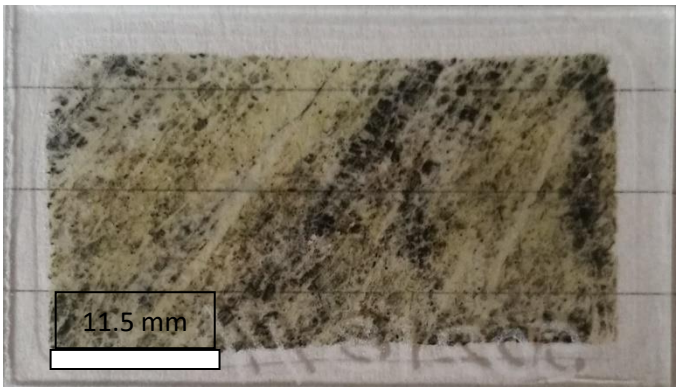

Figure 30: Sample 50218.14 thin-section

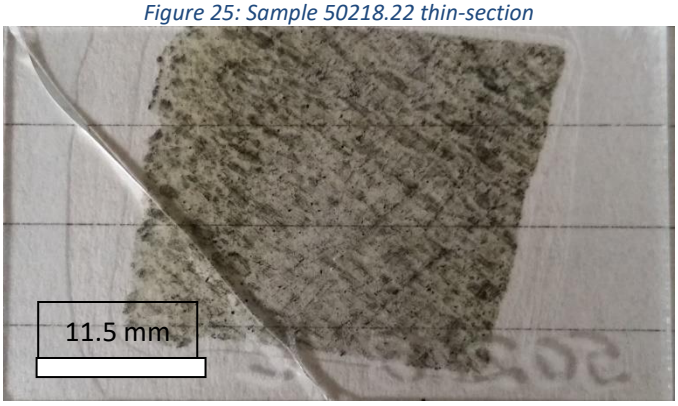

Figure 32: Sample 50218.1C thin-section

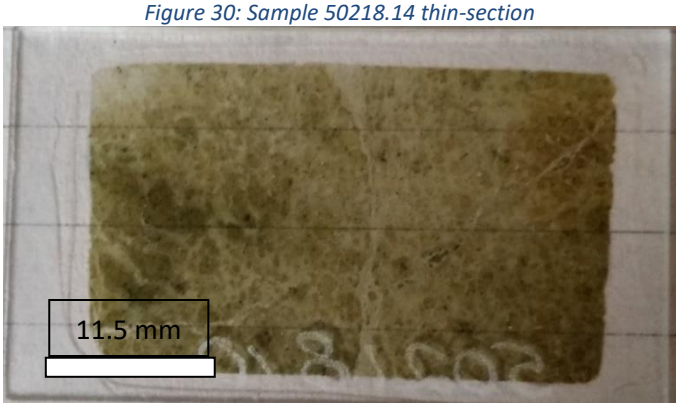

Figure 19: Sample 50218.10 thin-section

Appendix 2: XRF Images

XRF images were collected by Bruker using an M4 Tornado and by the Colorado School of Mines.

Presque Isle Peridotite

Section i: Sample 43018.1B

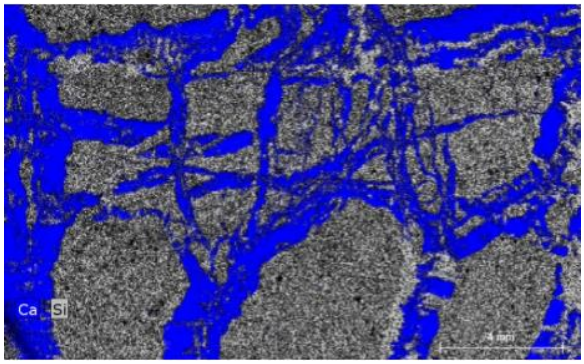

Figure 13: XRF image showing the distribution of Ca and Si in sample 43018.1B

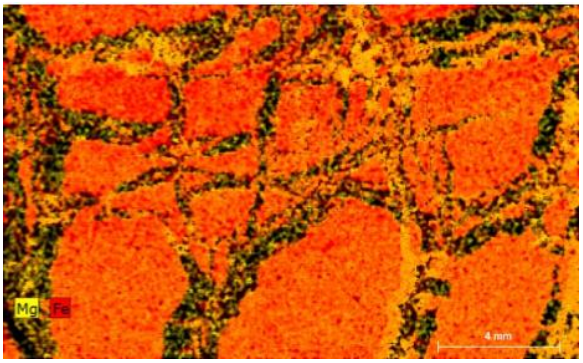

Figure 12: XRF image showing the distribution of Mg and Fe in sample 43018.1B

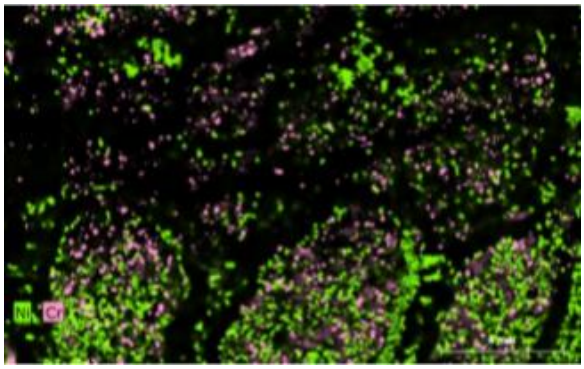

Figure 43: XRF image showing the distribution of Ni and Cr in sample 43018.1B

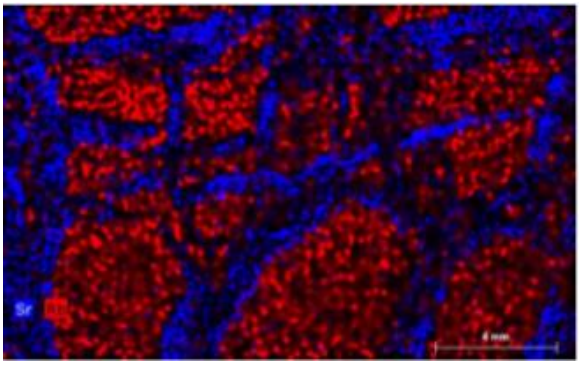

Figure 44: XRF image showing the distribution of Sr and Rb in sample 43018.1B

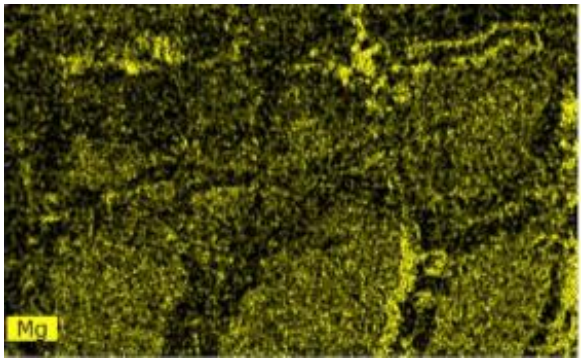

Figure 45: XRF image showing the distribution of Mg in sample 43018.1B

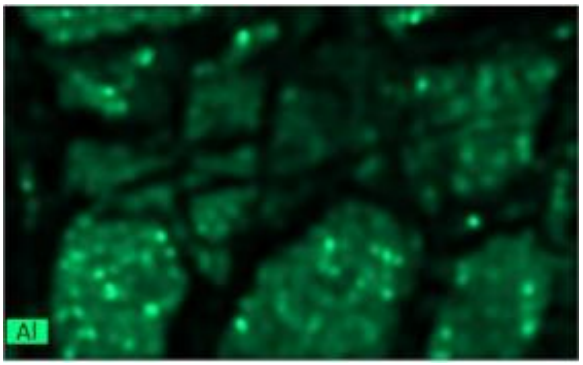

Figure 46: XRF image showing the distribution of Al in sample 43018.1B

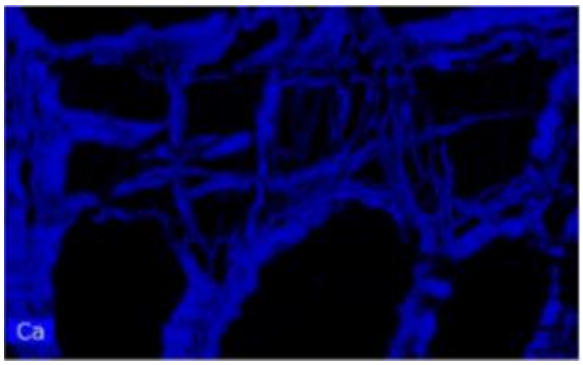

Figure 47: XRF image showing the distribution of Ca in sample 43018.1B

Figure 48: XRF image showing the distribution of Fe in sample 43018.1B

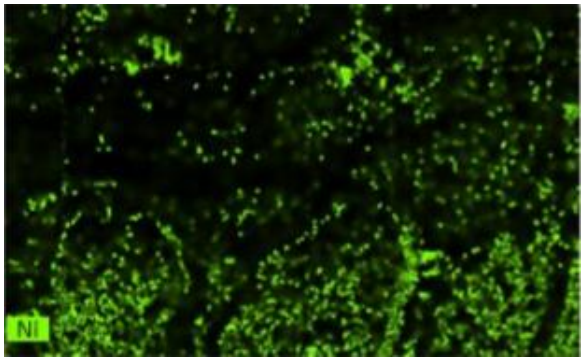

Figure 49: XRF image showing the distribution of Ni in sample 43018.1B

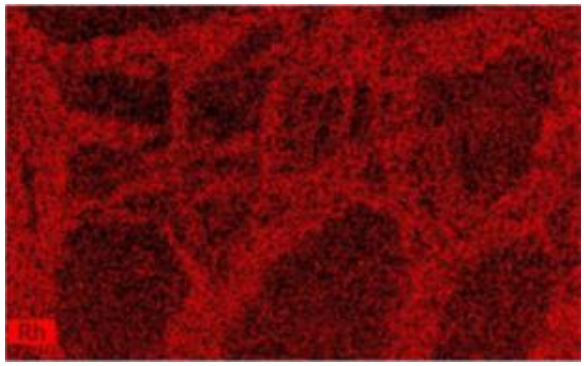

Figure 50: XRF image showing the distribution of Rh in sample 43018.1B

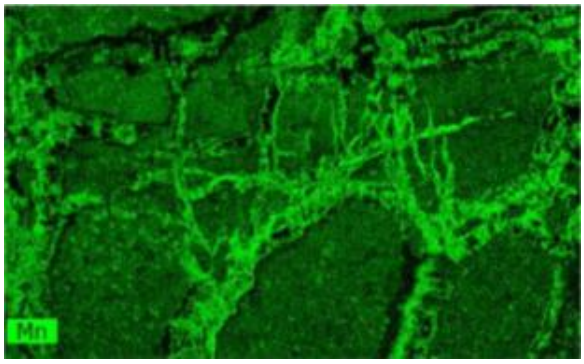

Figure 51: XRF image showing the distribution of Mn in sample 43018.1B

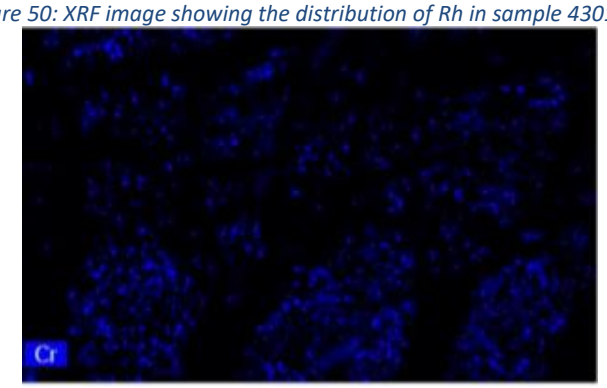

Figure 52: XRF image showing the distribution of Cr in sample 43018.1B

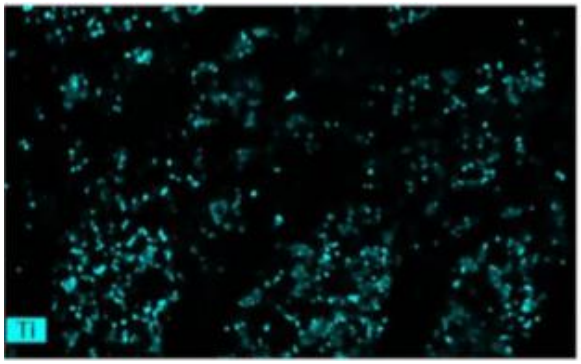

Figure 53: XRF image showing the distribution of Ti in sample 43018.1B

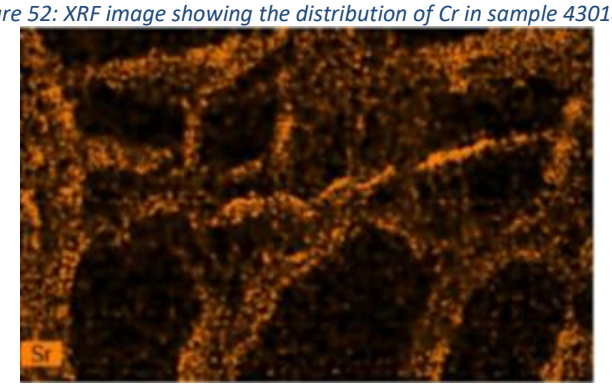

Figure 54: XRF image showing the distribution of Sr in sample 43018.1B

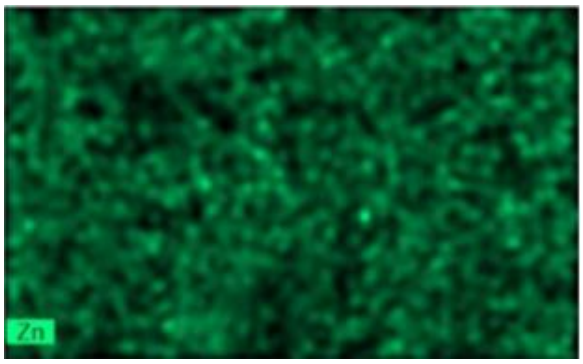

Figure 55: XRF image showing the distribution of Zn in sample 43018.1B

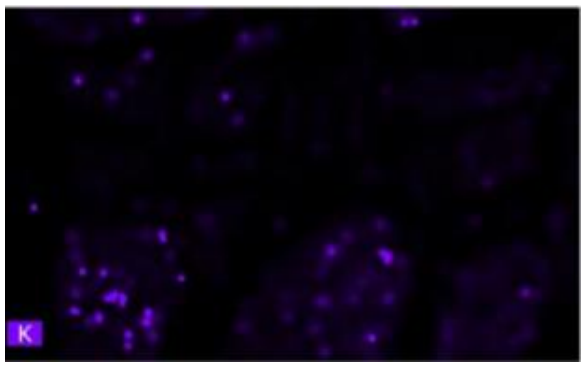

Figure 56: XRF image showing the distribution of K in sample 43018.1B

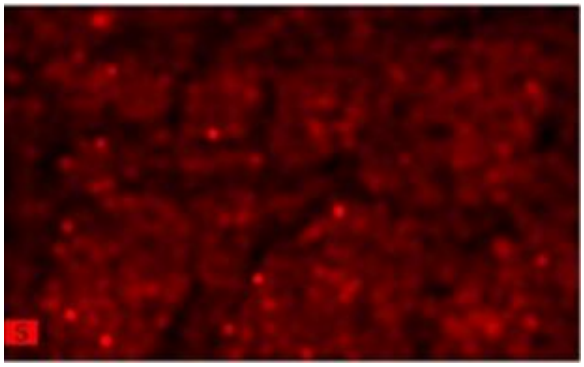

Figure 57: XRF image showing the distribution of S in sample 43018.1B

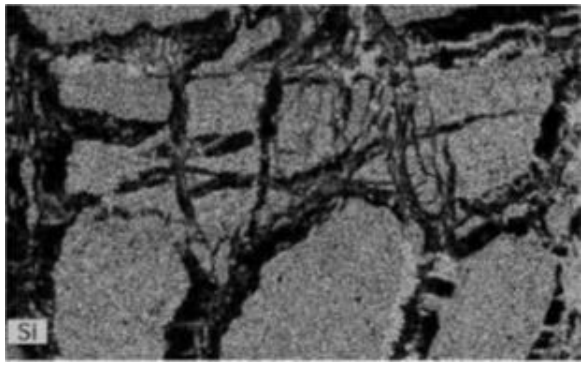

Figure 58: XRF image showing the distribution of Si in sample 43018.1B

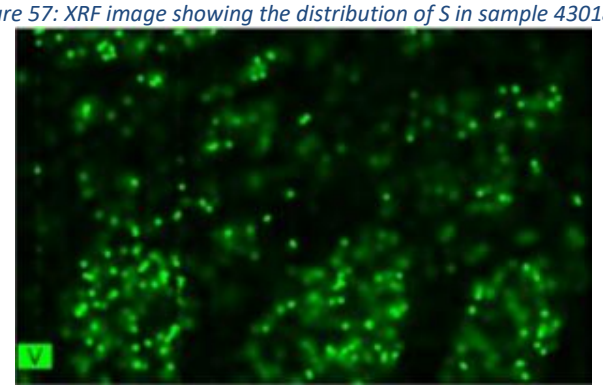

Figure 59: XRF image showing the distribution of V in sample 43018.1B

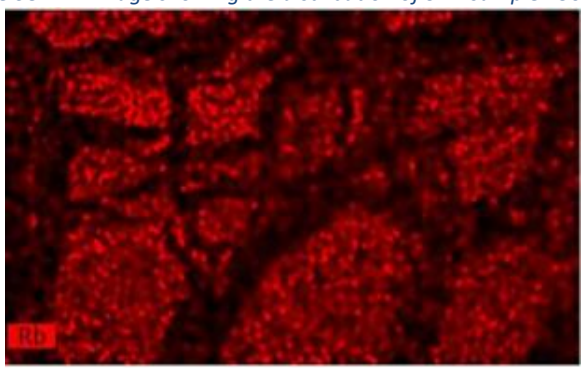

Figure 60: XRF image showing the distribution of Rb in sample 43018.1B

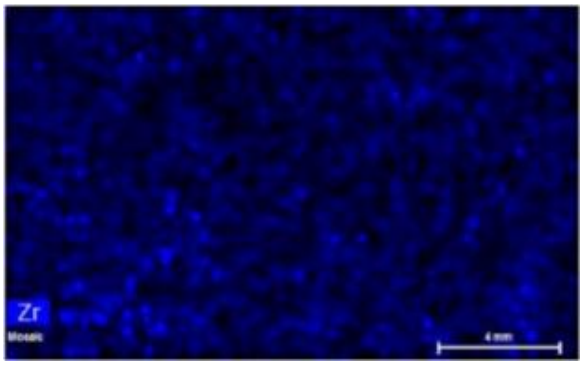

Figure 61: XRF image showing the distribution of Zr in sample 43018.1B

Section ii: Sample 43018.1

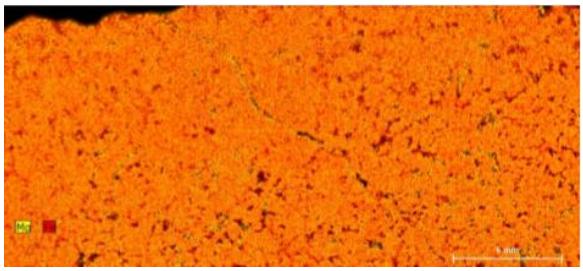

Figure 17: XRF image showing the distribution of Mg and Fe in sample 43018.1

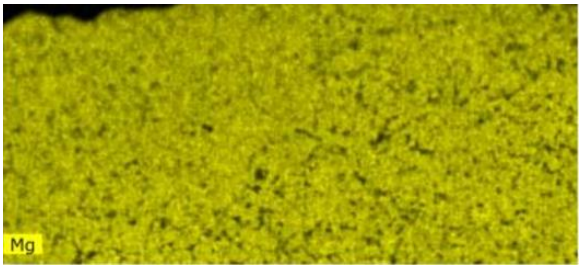

Figure 62: XRF image showing the distribution of Mg in sample 43018.1

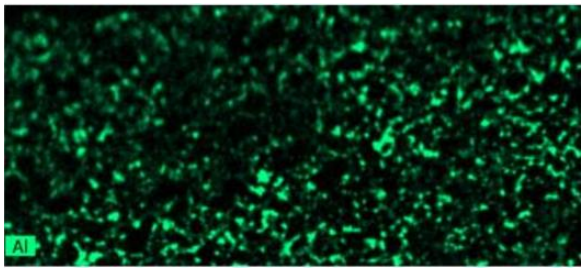

Figure 63: XRF image showing the distribution of Al in sample 43018.1

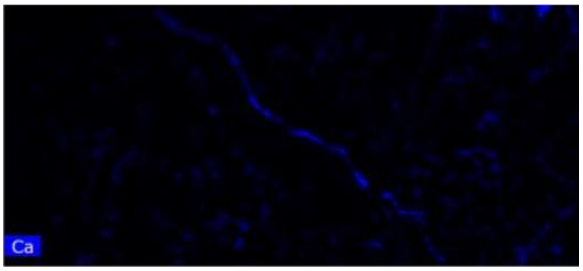

Figure 18: XRF image showing the distribution of Ca in sample 43018.1

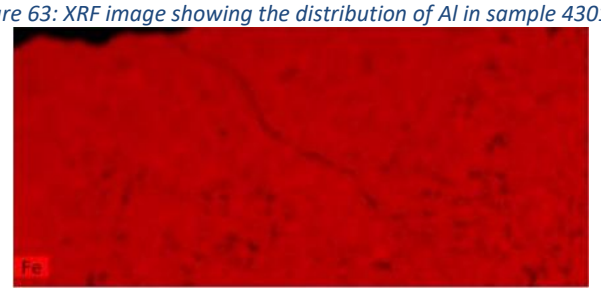

Figure 64: XRF image showing the distribution of Fe in sample 43018.1

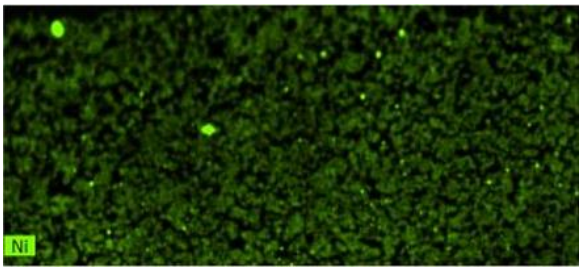

Figure 65: XRF image showing the distribution of Ni in sample 43018.1

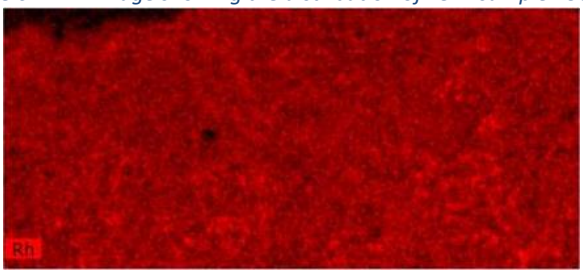

Figure 67: XRF image showing the distribution of Rh in sample 43018.1

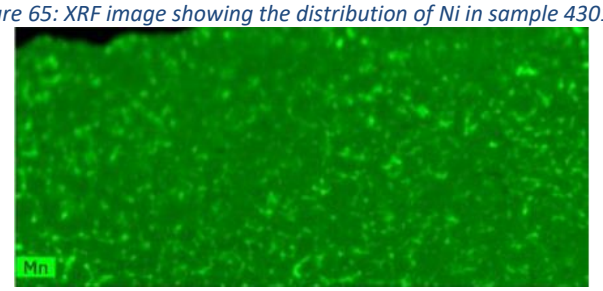

Figure 68: XRF image showing the distribution of Mn in sample 43018.1

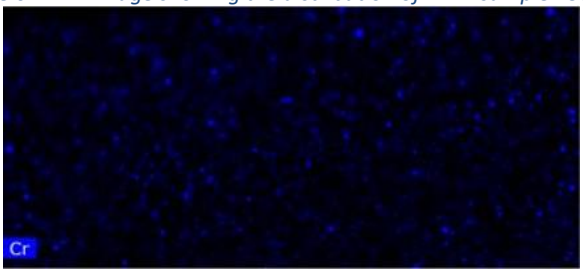

Figure 69: XRF image showing the distribution of Cr in sample 43018.1

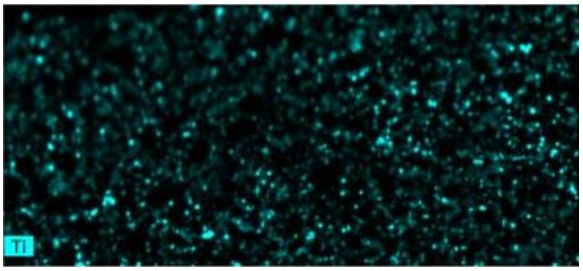

Figure 70: XRF image showing the distribution of Ti in sample 43018.1

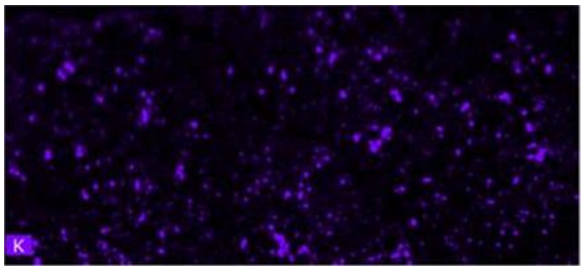

Figure 71: XRF image showing the distribution of K in sample 43018.1

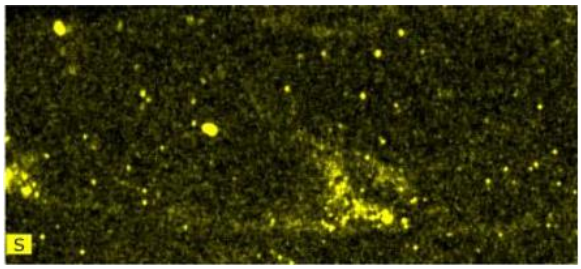

Figure 72: XRF image showing the distribution of S in sample 43018.1

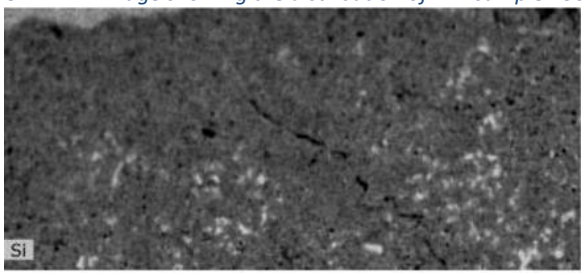

Figure 73: XRF image showing the distribution of Si in sample 43018.1

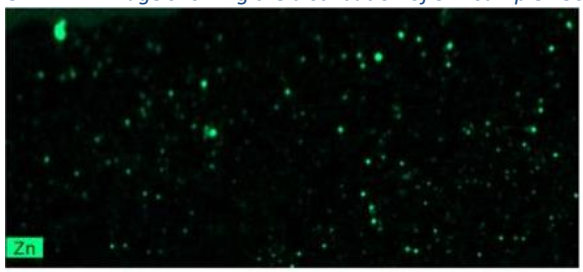

Figure 74: XRF image showing the distribution of Zn in sample 43018.1

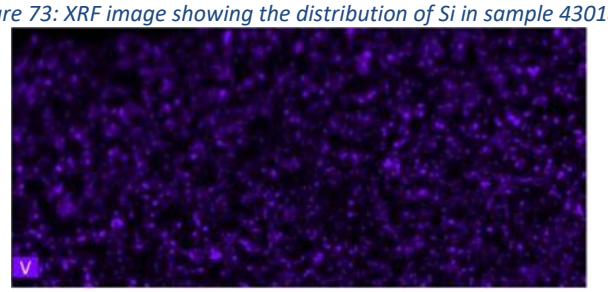

Figure 75: XRF image showing the distribution of V in sample 43018.1

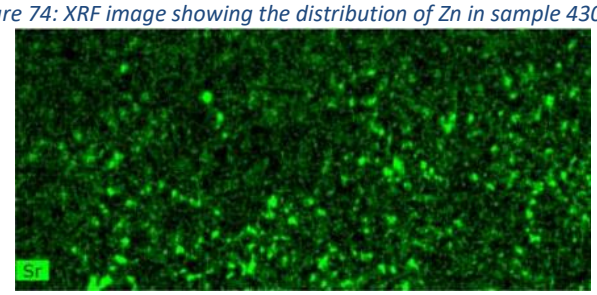

Figure 76: XRF image showing the distribution of Sr in sample 43018.1

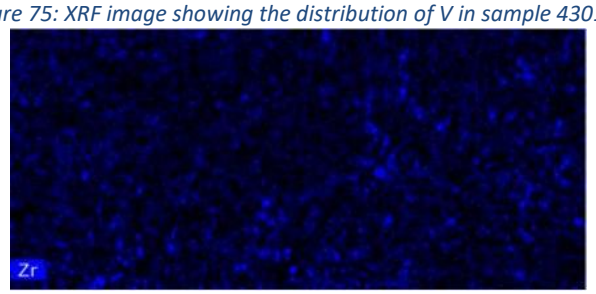

Figure 77: XRF image showing the distribution of Zr in sample 43018.1

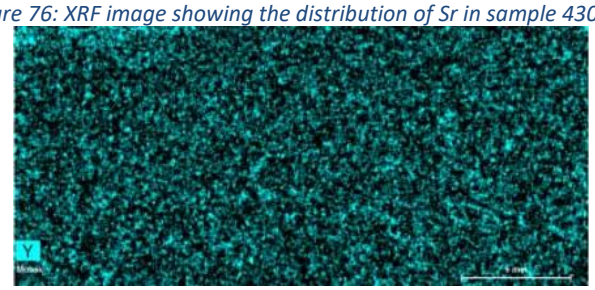

Figure 78: XRF image showing the distribution of Y in sample 43018.1

Deer Lake Peridotite

Section iii: Sample 50218.1B (Bruker Data)

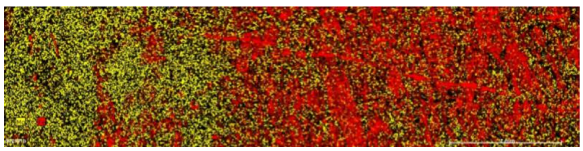

Figure 79: XRF image showing the distribution of Mg and Fe in sample 50218.1B

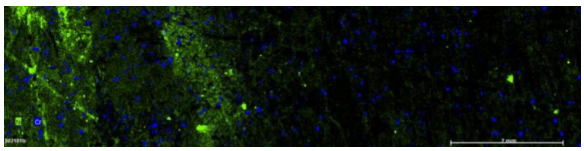

Figure 80: XRF image showing the distribution of Ni and Cr in sample 50218.1B

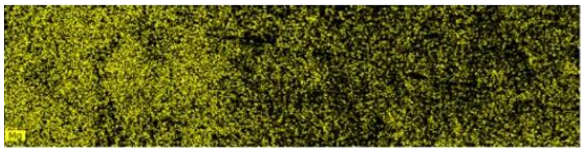

Figure 81: XRF image showing the distribution of Mg in sample 50218.1B

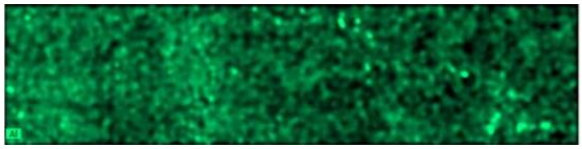

Figure 82: XRF image showing the distribution of Al in sample 50218.1B

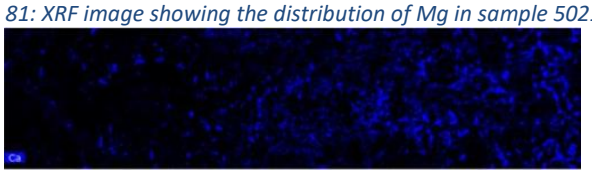

Figure 83: XRF image showing the distribution of Ca in sample 50218.1B

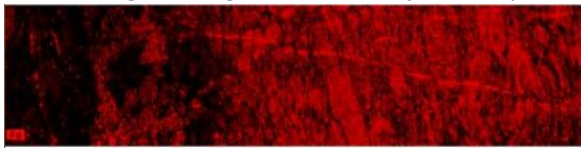

Figure 84: XRF image showing the distribution of Fe in sample 50218.1B

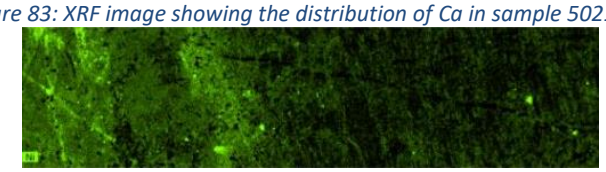

Figure 85: XRF image showing the distribution of Ni in sample 50218.1B

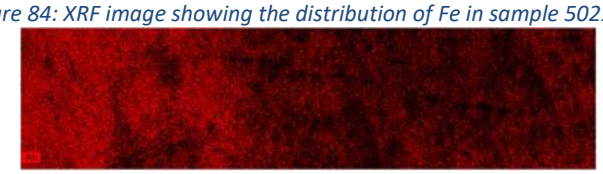

Figure 86: XRF image showing the distribution of Rh in sample 50218.1B

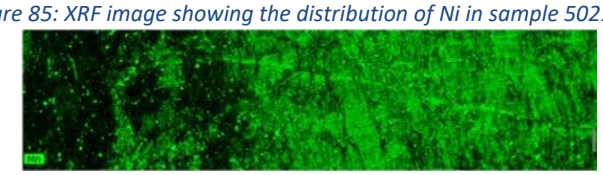

Figure 87: XRF image showing the distribution of Mn in sample 50218.1B

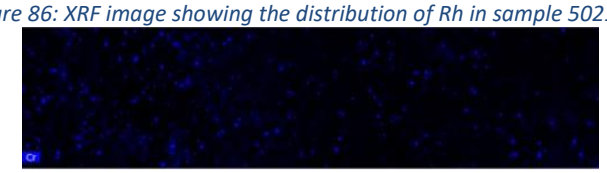

Figure 88: XRF image showing the distribution of Cr in sample 50218.1B

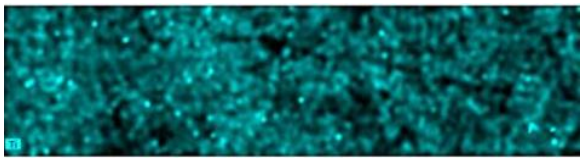

Figure 89: XRF image showing the distribution of Ti in sample 50218.1B

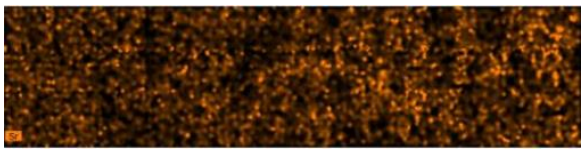

Figure 90: XRF image showing the distribution of Sr in sample 50218.1B

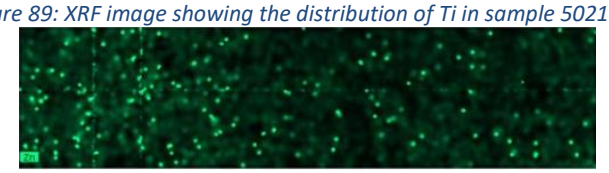

Figure 91: XRF image showing the distribution of Zn in sample 50218.1B

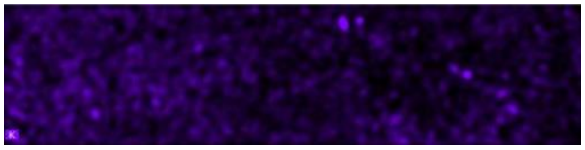

Figure 92: XRF image showing the distribution of K in sample 50218.1B

Figure 93: XRF image showing the distribution of S in sample 50218.1B

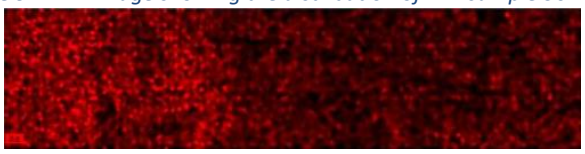

Figure 94: XRF image showing the distribution of As in sample 50218.1B

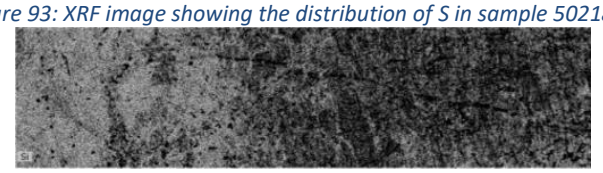

Figure 95: XRF image showing the distribution of Si in sample 50218.1B

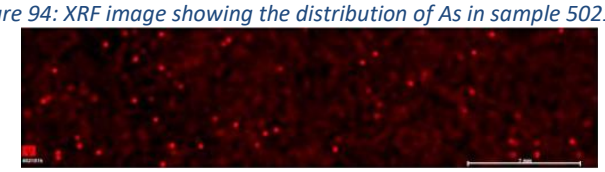

Figure 96: XRF image showing the distribution of V in sample 50218.1B

Section iv: Sample 50218.1B (Colorado School of Mines Data)

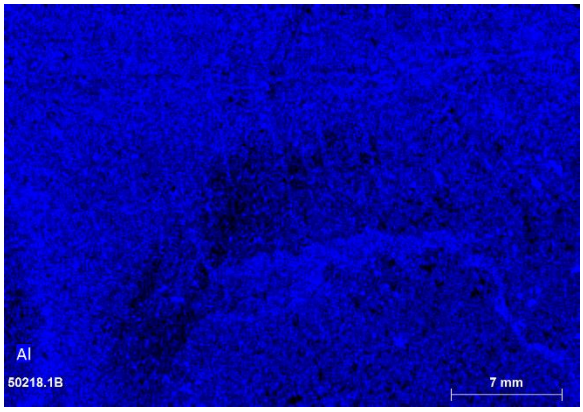

Figure 97: XRF image showing the distribution of Al in sample 50218.1B

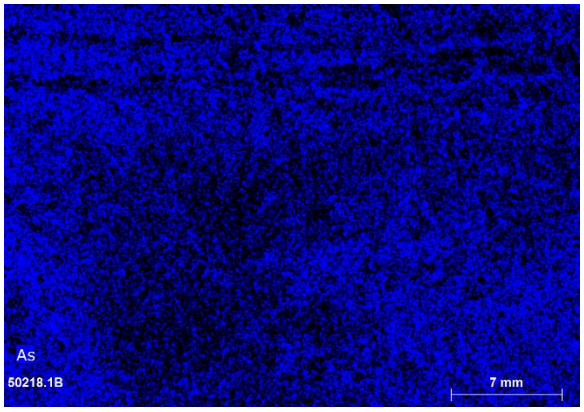

Figure 98: XRF image showing the distribution of As in sample 50218.1B

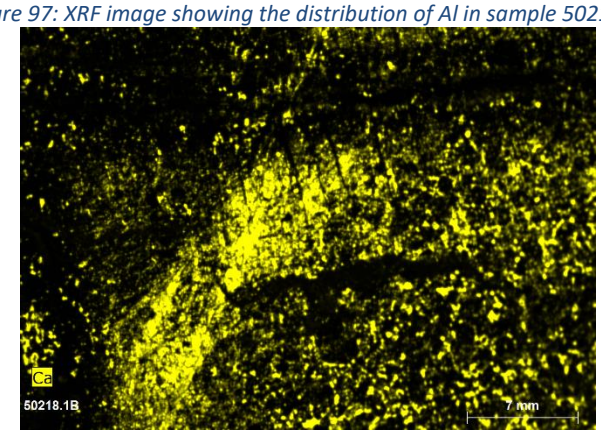

Figure 99: XRF image showing the distribution of Ca in sample 50218.1B

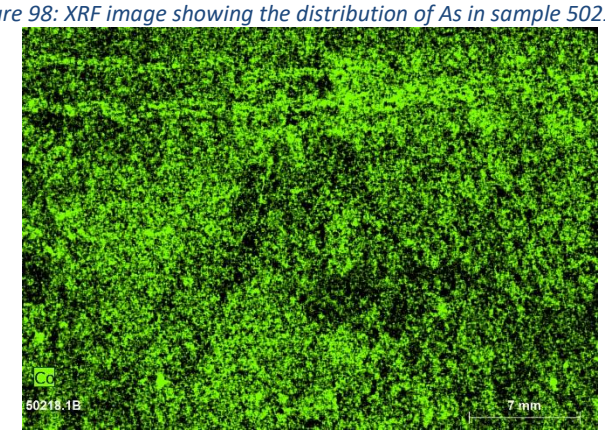

Figure 100: XRF image showing the distribution of Co in sample 50218.1B

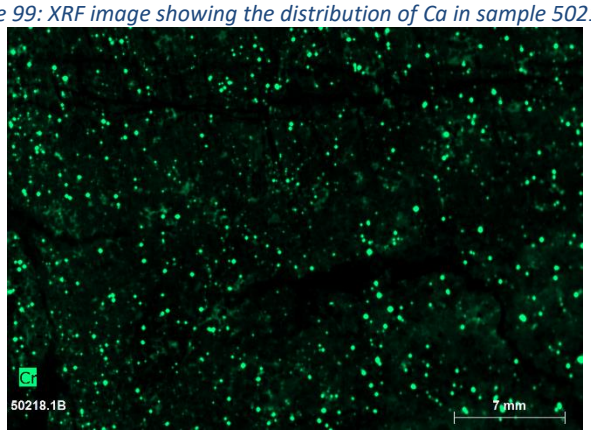

Figure 101: XRF image showing the distribution of Cr in sample 50218.1B

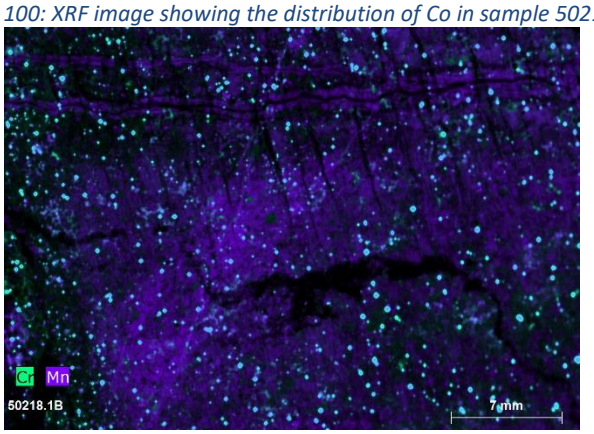

Figure 102: XRF image showing the distribution of Cr and Mn in sample 50218.1B

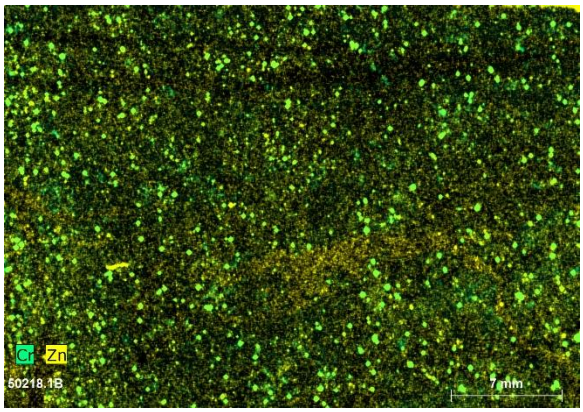

Figure 103: XRF image showing the distribution of Cr and Zn in sample 50218.1B

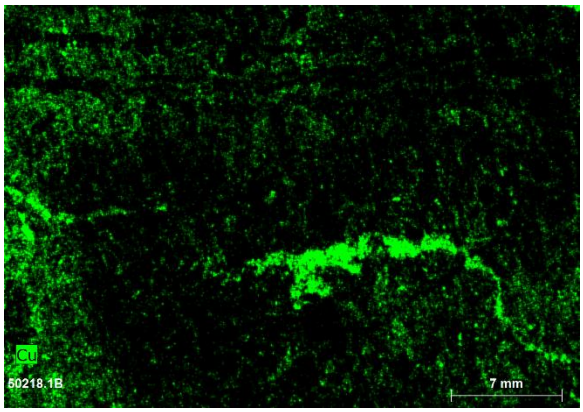

Figure 104: XRF image showing the distribution of Cu in sample 50218.1B

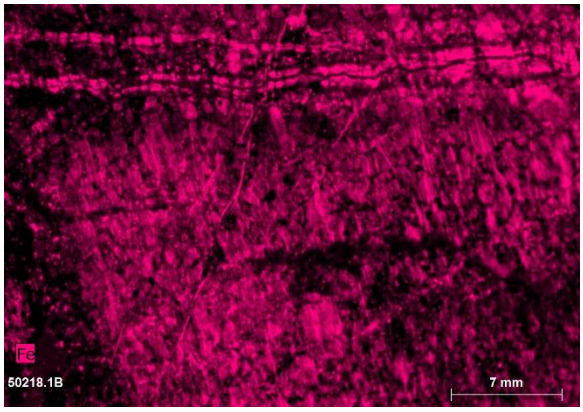

Figure 105: XRF image showing the distribution of Fe in sample 50218.1B

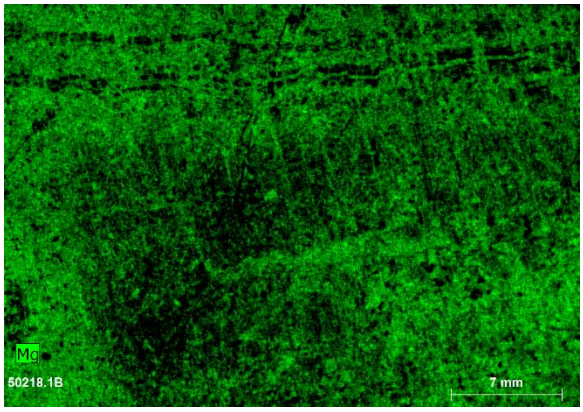

Figure 106: XRF image showing the distribution of Mg in sample 50218.1B

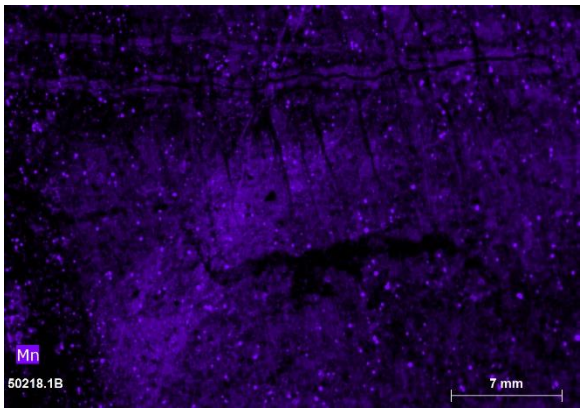

Figure 107: XRF image showing the distribution of Mn in sample 50218.1B

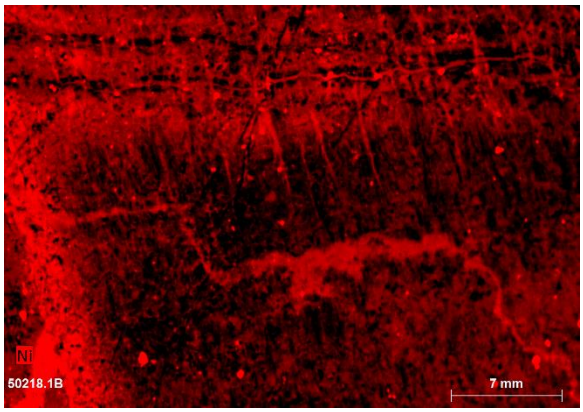

Figure 108: XRF image showing the distribution of Ni in sample 50218.1B

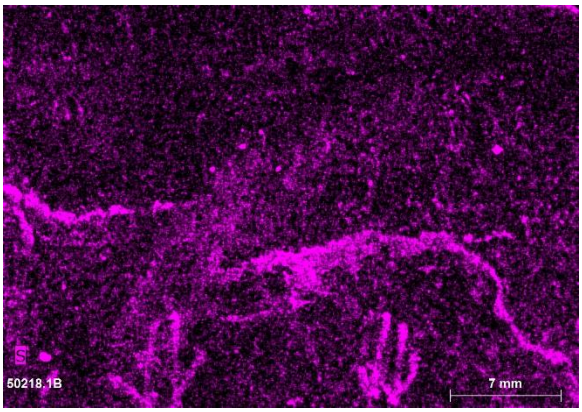

Figure 109: XRF image showing the distribution of S in sample 50218.1B

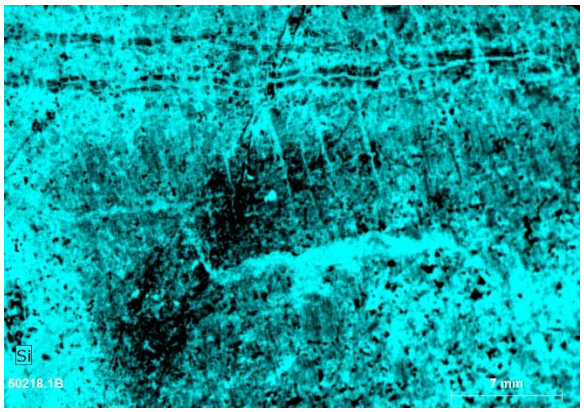

Figure 110: XRF image showing the distribution of Si in sample 50218.1B

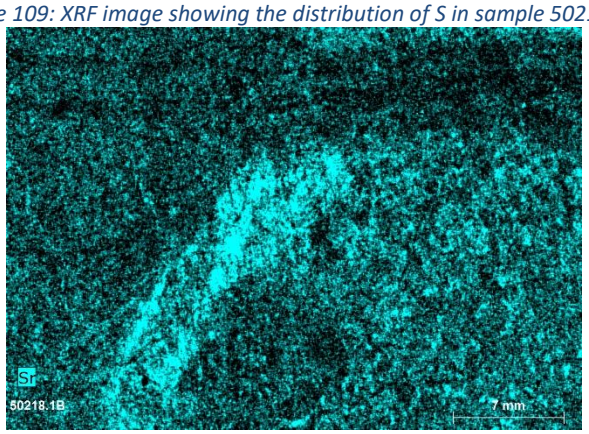

Figure 111: XRF image showing the distribution of Sr in sample 50218.1B

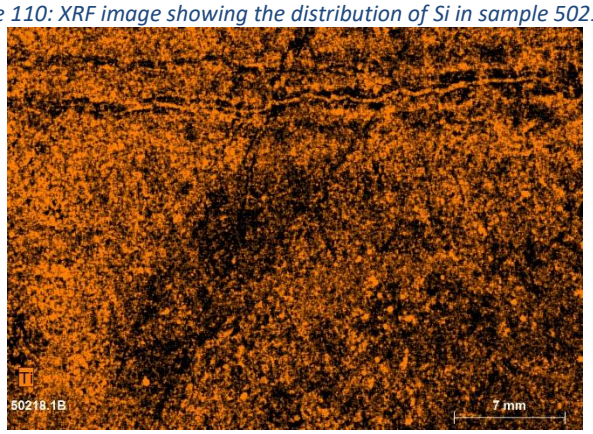

Figure 112: XRF image showing the distribution of Ti in sample 50218.1B

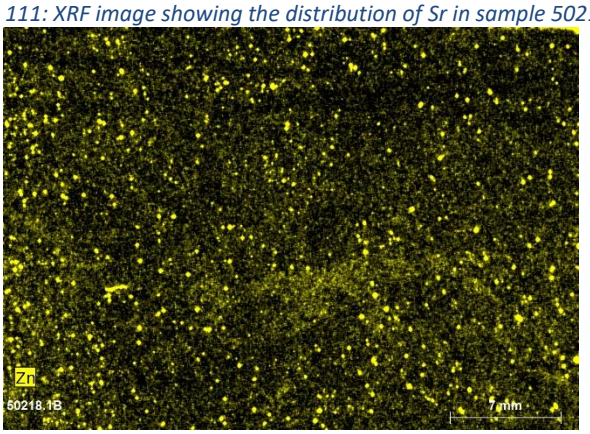

Figure 113: XRF image showing the distribution of Zn in sample 50218.1B

Section v: Sample 50218.3A

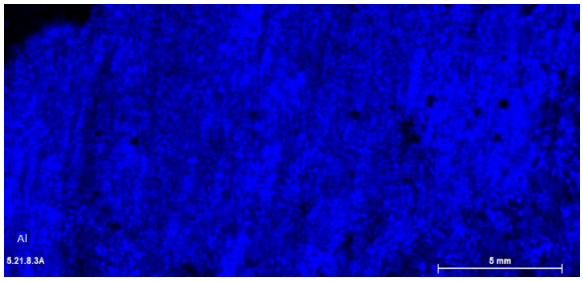

Figure 114: XRF image showing the distribution of Al in sample 50218.3A

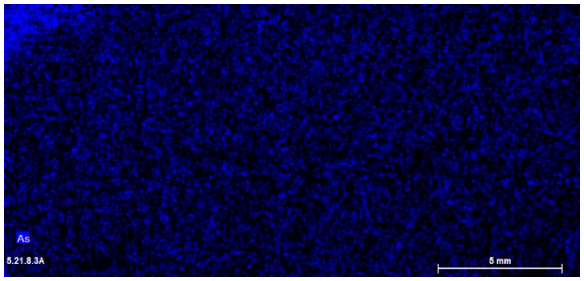

Figure 115: XRF image showing the distribution of As in sample 50218.3A

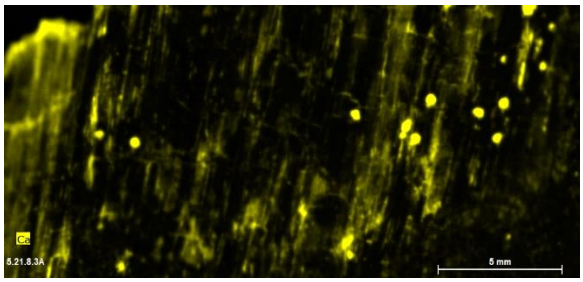

Figure 35: XRF image showing the distribution of Ca in sample 50218.3A

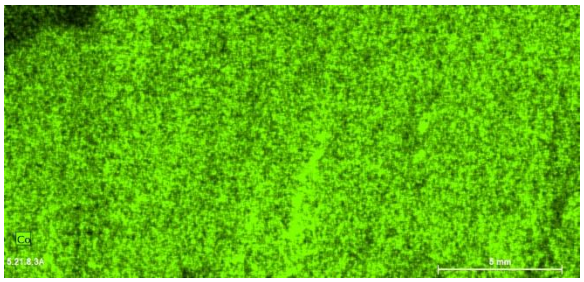

Figure 116: XRF image showing the distribution of Co in sample 50218.3A

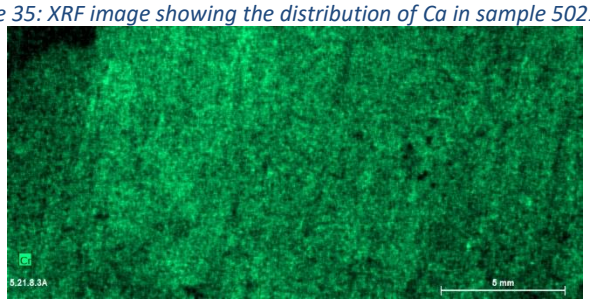

Figure 117: XRF image showing the distribution of Cr in sample 50218.3A

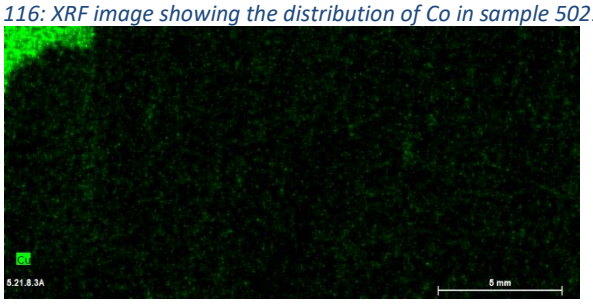

Figure 118: XRF image showing the distribution of Cu in sample 50218.3A

Figure 119: XRF image showing the distribution of Fe in sample 50218.3A

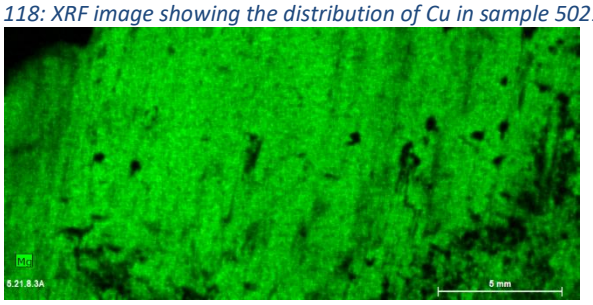

Figure 36: XRF image showing the distribution of Mg in sample 50218.3A

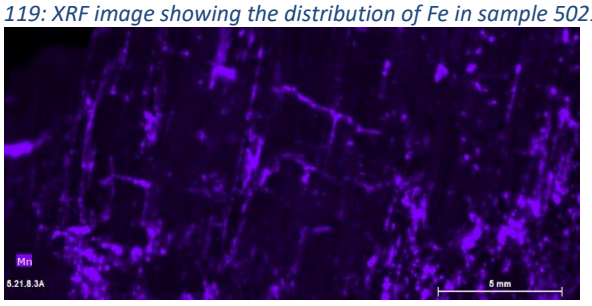

Figure 120: XRF image showing the distribution of Mn in sample 50218.3A

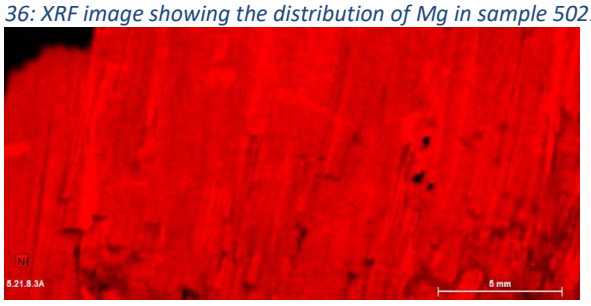

Figure 121: XRF image showing the distribution of Ni in sample 50218.3A

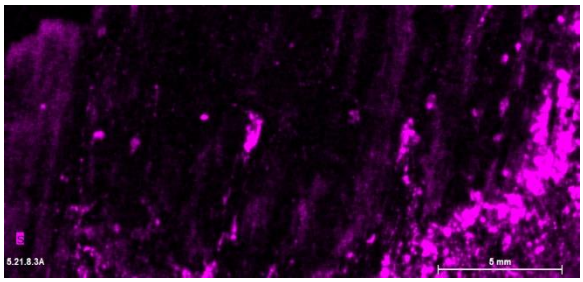

Figure 122: XRF image showing the distribution of S in sample 50218.3A

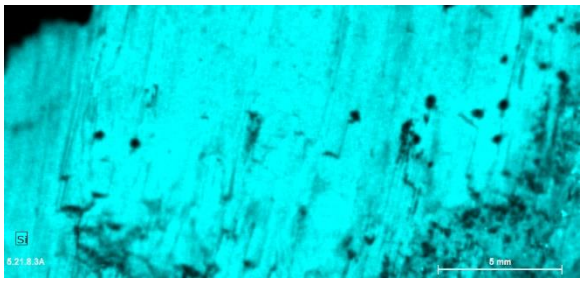

Figure 123: XRF image showing the distribution of Si in sample 50218.3A

Figure 124: XRF image showing the distribution of Sr in sample 50218.3A

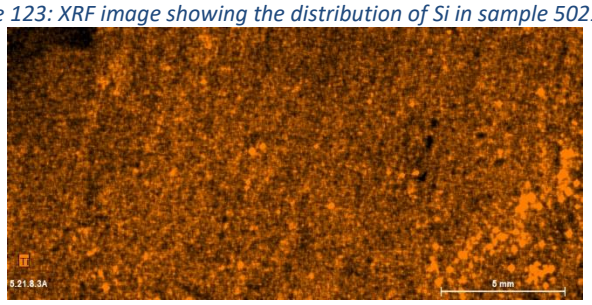

Figure 125: XRF image showing the distribution of Ti in sample 50218.3A

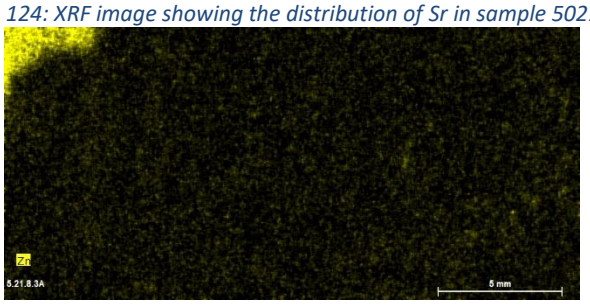

Figure 126: XRF image showing the distribution of Zn in sample 50218.3A

Section vi: Sample 501218.22

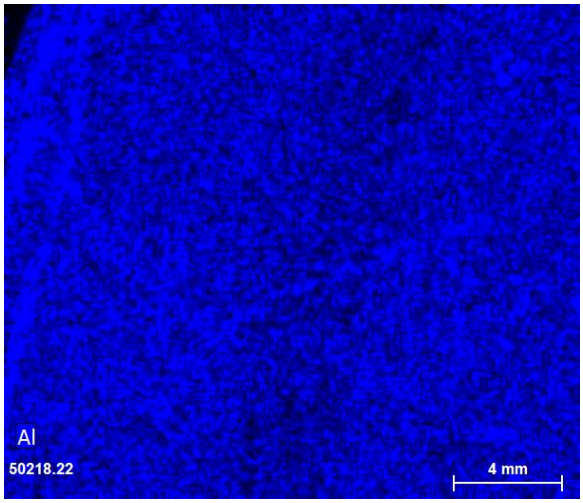

Figure 127: XRF image showing the distribution of Al in sample 501218.22

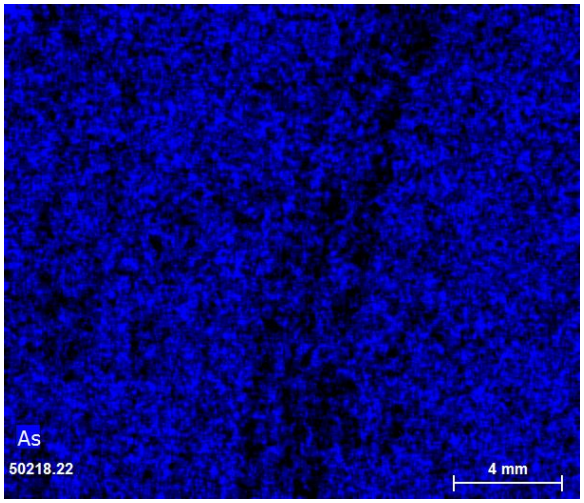

Figure 128: XRF image showing the distribution of As in sample 501218.22

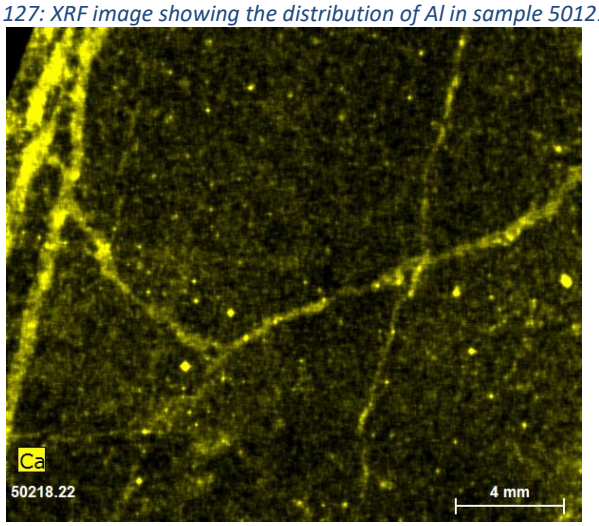

Figure 27: XRF image showing the distribution of Ca in sample 501218.22

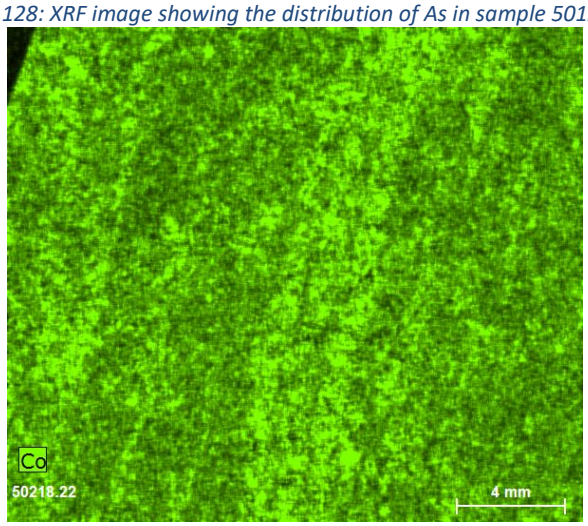

Figure 129: XRF image showing the distribution of Co in sample 501218.22

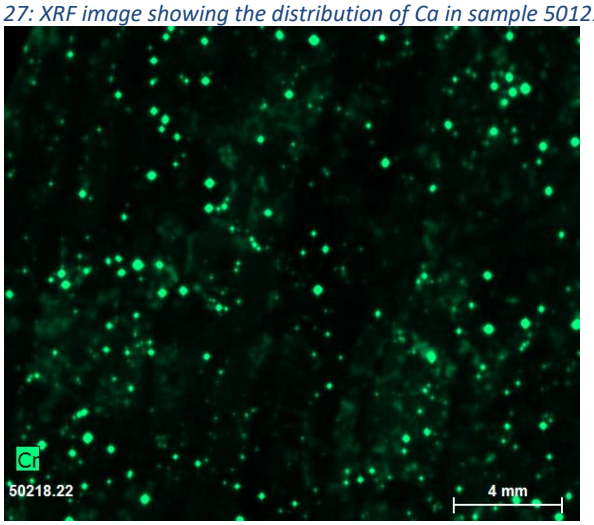

Figure 130: XRF image showing the distribution of Cr in sample 501218.22

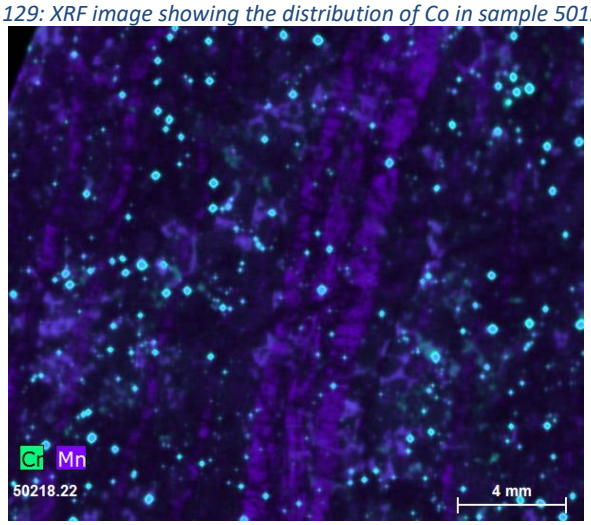

Figure 131: XRF image showing the distribution of Cr and Mn in sample 501218.22

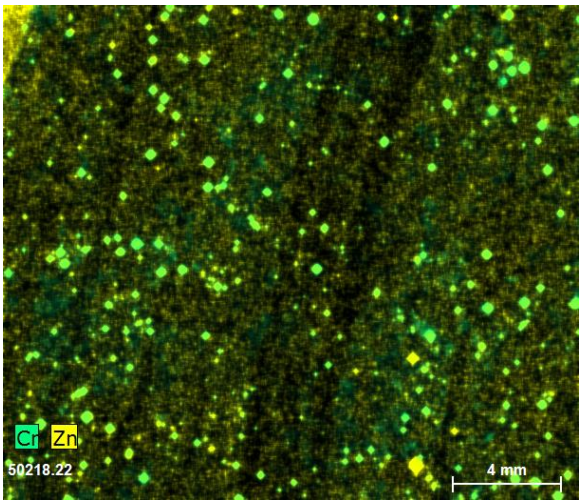

Figure 132: XRF image showing the distribution of Cr and Zn in sample 501218.22

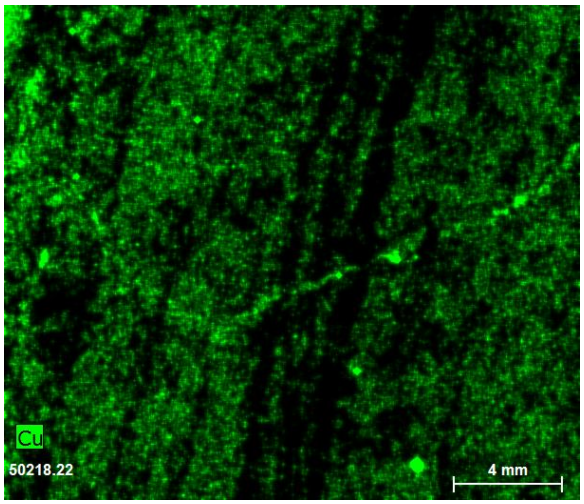

Figure 29: XRF image showing the distribution of Cu in sample 501218.22

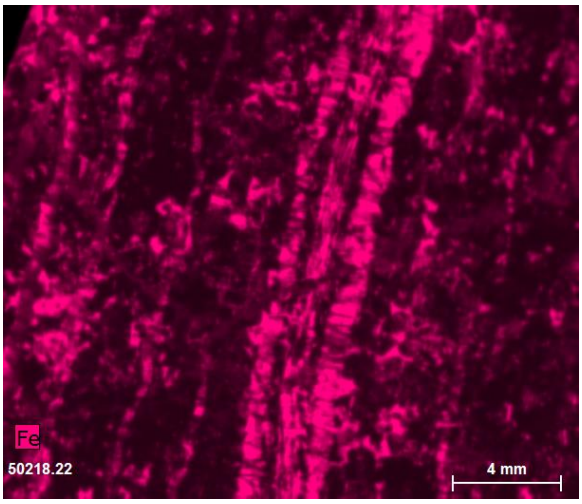

Figure 26: XRF image showing the distribution of Fe in sample 501218.22

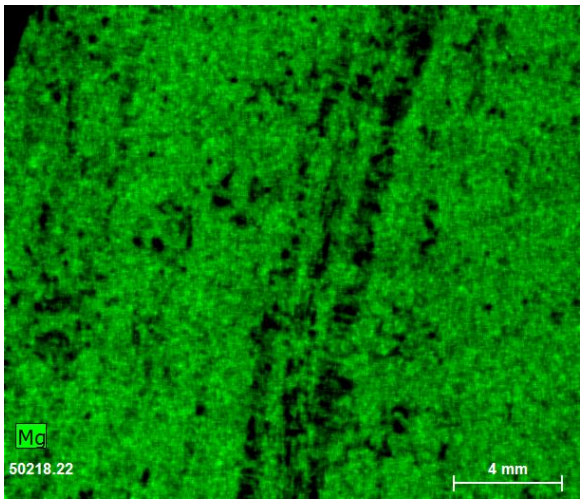

Figure 133: XRF image showing the distribution of Mg in sample 501218.22

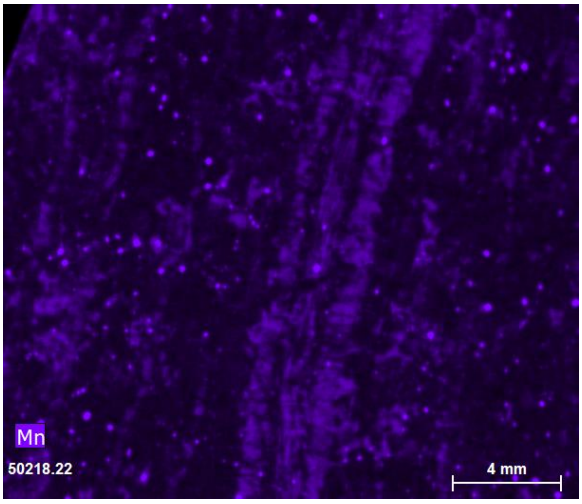

Figure 134: XRF image showing the distribution of Mn in sample 501218.22

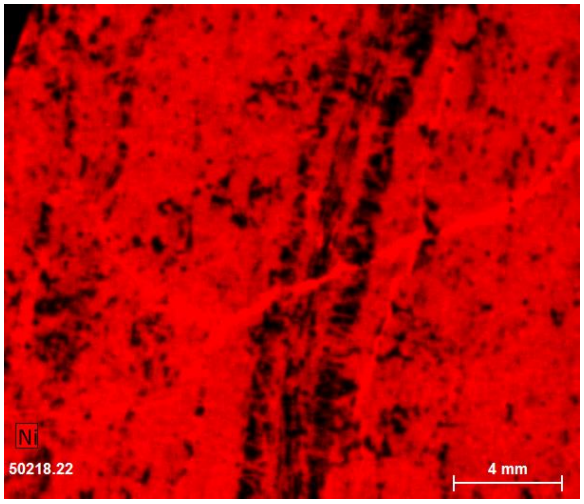

Figure 135: XRF image showing the distribution of Ni in sample 501218.22

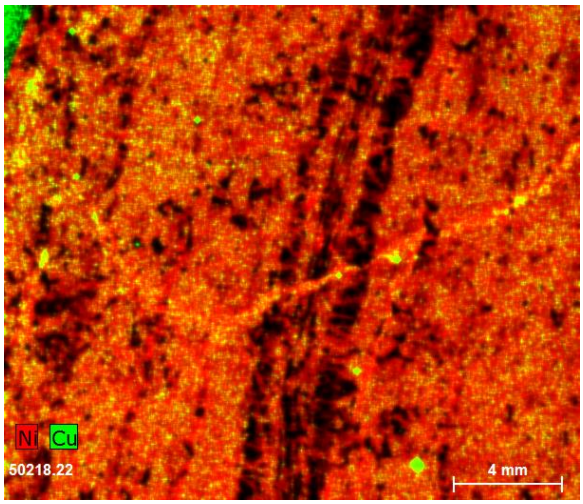

Figure 136: XRF image showing the distribution of Ni and Cu in sample 501218.22

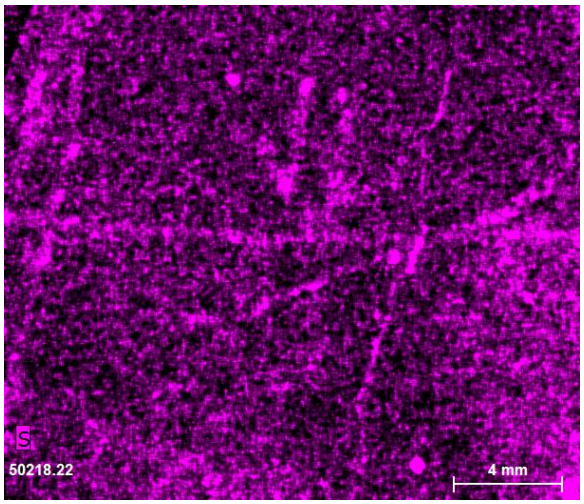

Figure 137: XRF image showing the distribution of S in sample 501218.22

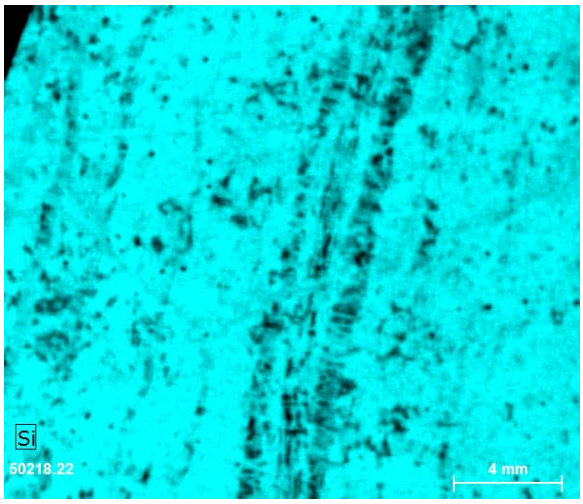

Figure 138: XRF image showing the distribution of Si in sample 501218.22

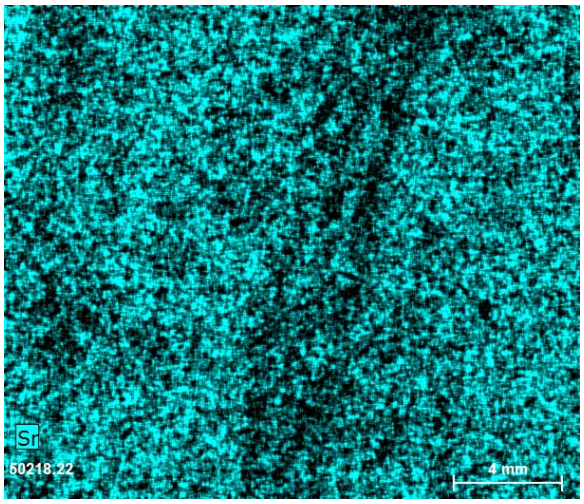

Figure 139: XRF image showing the distribution of Sr in sample 501218.22

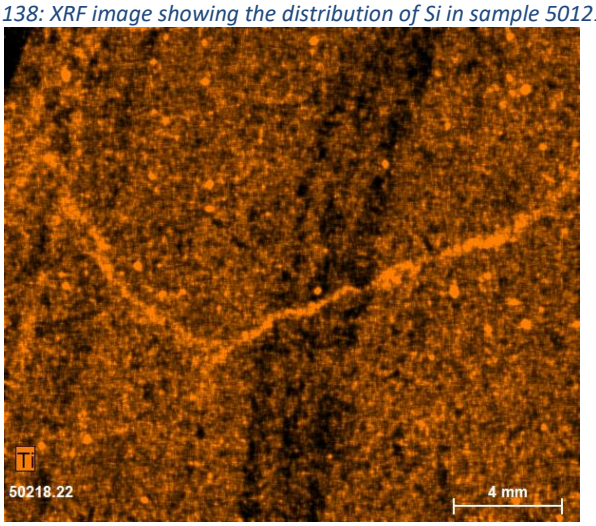

Figure 28: XRF image showing the distribution of Ti in sample 501218.22

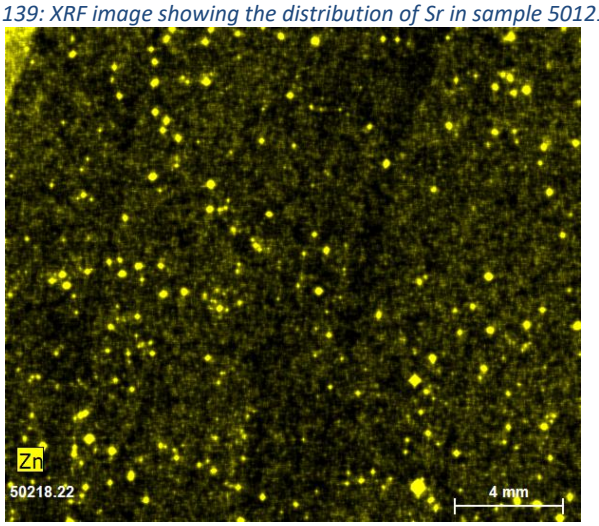

Figure 140: XRF image showing the distribution of Zn in sample 501218.22

Section vii: Sample 50218.14

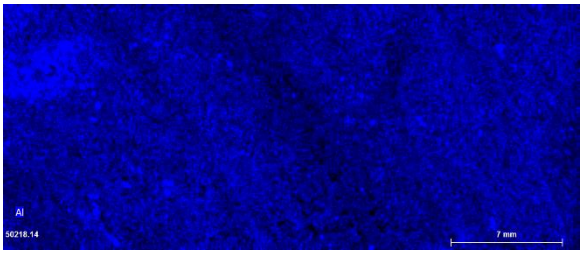

Figure 141: XRF image showing the distribution of Al in sample 50218.14

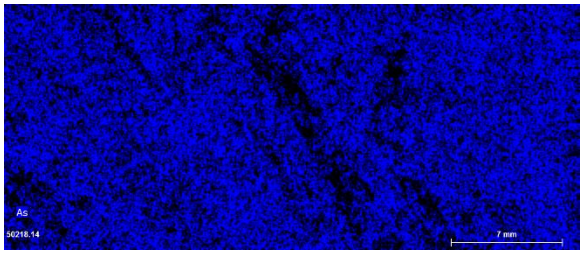

Figure 142: XRF image showing the distribution of As in sample 50218.14

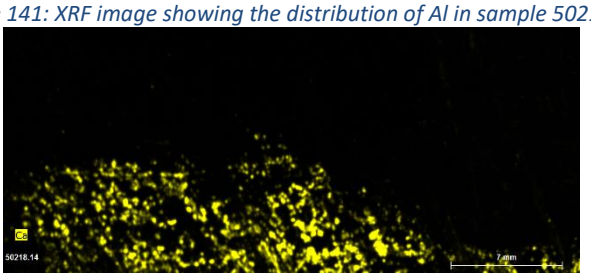

Figure 143: XRF image showing the distribution of Ca in sample 50218.14

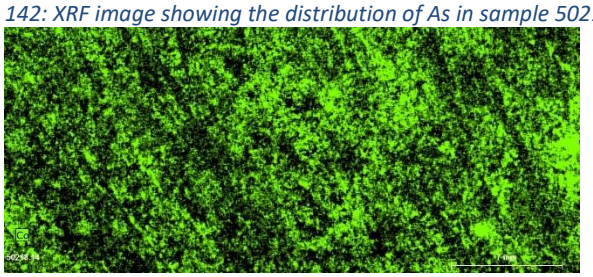

Figure 144: XRF image showing the distribution of Co in sample 50218.14

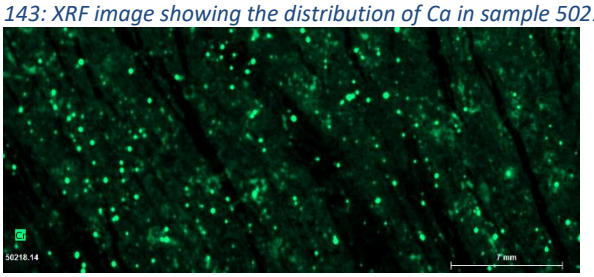

Figure 145: XRF image showing the distribution of Cr in sample 50218.14

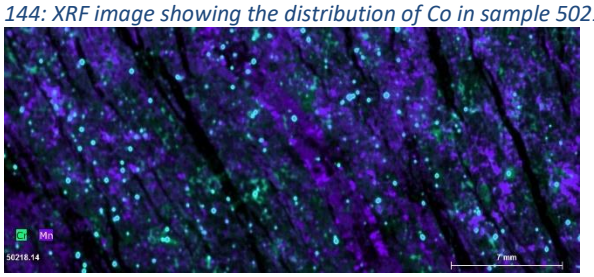

Figure 146: XRF image showing the distribution of Cr and Mn in sample 50218.14

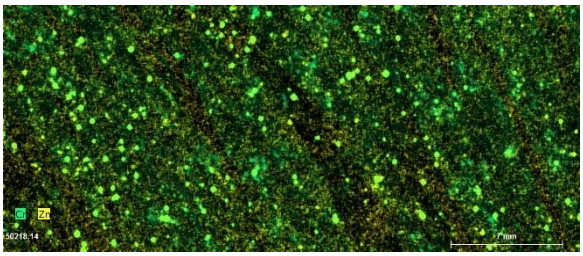

Figure 147: XRF image showing the distribution of Cr and Zn in sample 50218.14

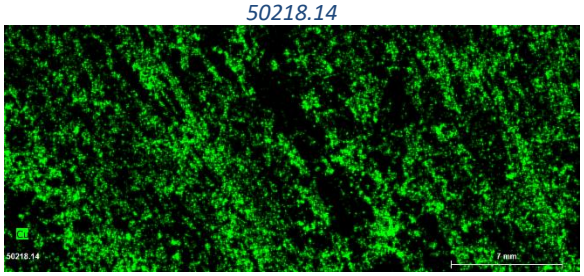

Figure 148: XRF image showing the distribution of Cu in sample 50218.14

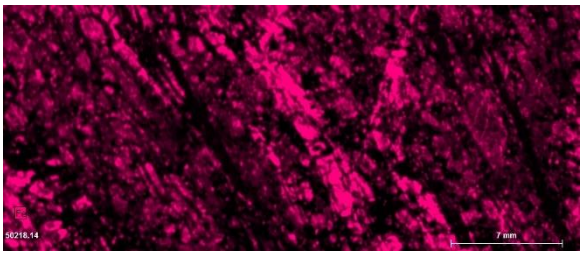

Figure 149: XRF image showing the distribution of Fe in sample 50218.14

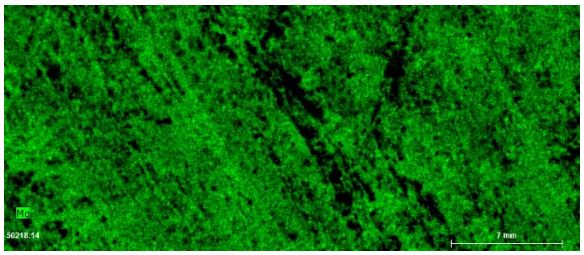

Figure 150: XRF image showing the distribution of Mg in sample 50218.14

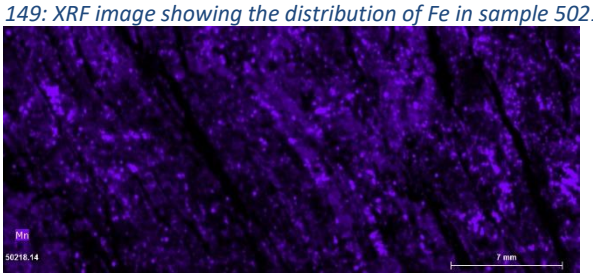

Figure 151: XRF image showing the distribution of Mn in sample 50218.14

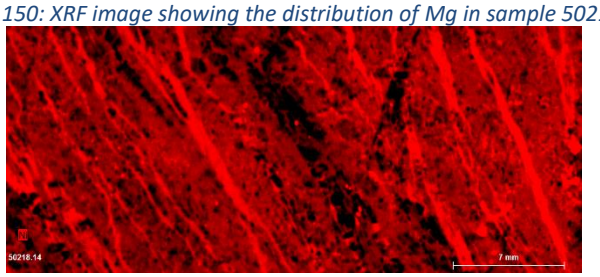

Figure 31: XRF image showing the distribution of Ni in sample 50218.14

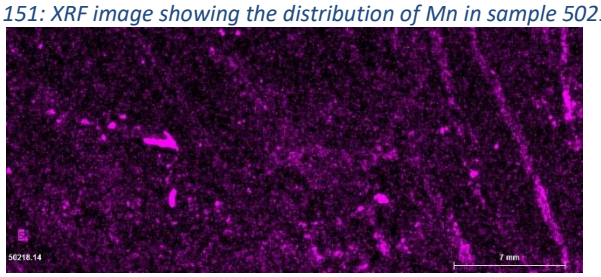

Figure 152: XRF image showing the distribution of S in sample 50218.14

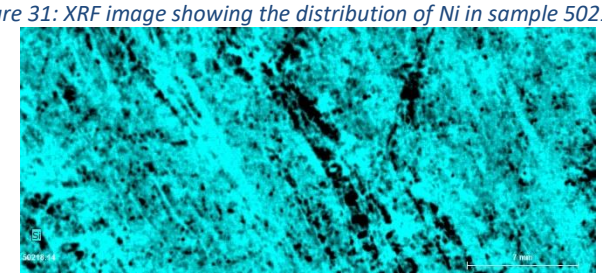

Figure 153: XRF image showing the distribution of Si in sample 50218.14

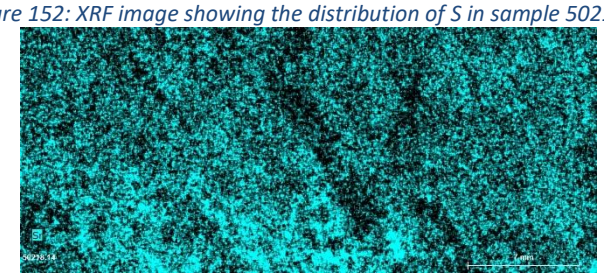

Figure 154: XRF image showing the distribution of Sr in sample 50218.14

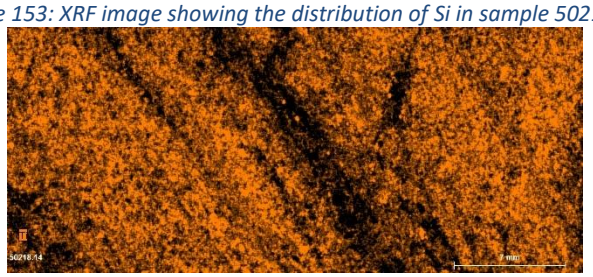

Figure 155: XRF image showing the distribution of Ti in sample 50218.14

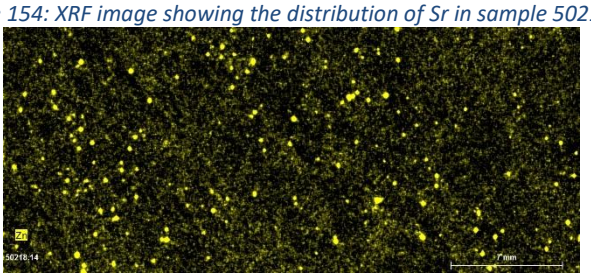

Figure 156: XRF image showing the distribution of Zn in sample 50218.14

Section viii: DL 5119.1

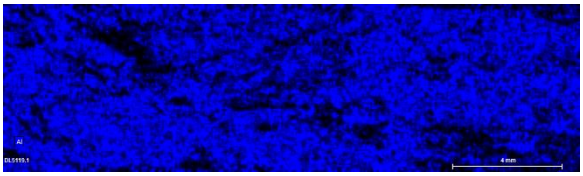

Figure 157: XRF image showing the distribution of Al in sample DL 5119.1

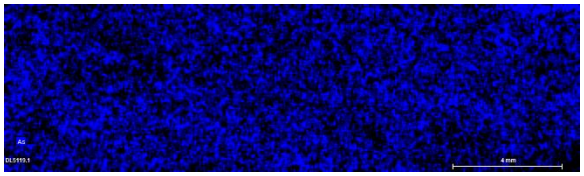

Figure 158: XRF image showing the distribution of As in sample DL 5119.1

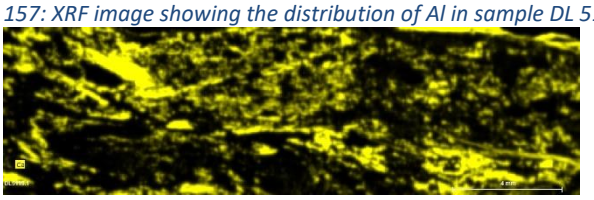

Figure 159: XRF image showing the distribution of Ca in sample DL 5119.1

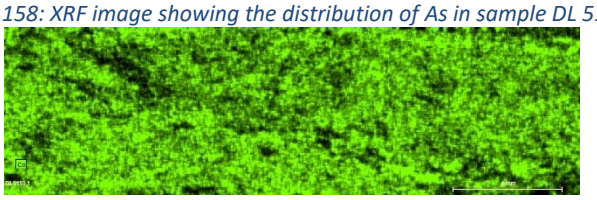

Figure 160: XRF image showing the distribution of Co in sample DL 5119.1

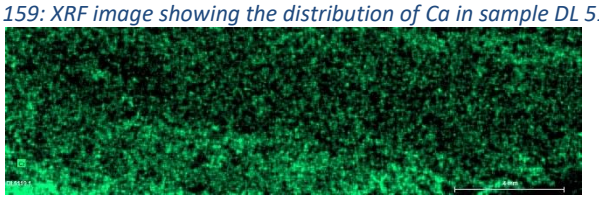

Figure 161: XRF image showing the distribution of Cr in sample DL 5119.1

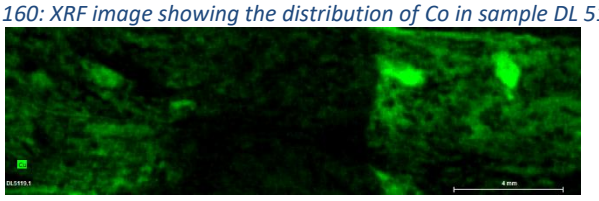

Figure 162: XRF image showing the distribution of Cu in sample DL 5119.1

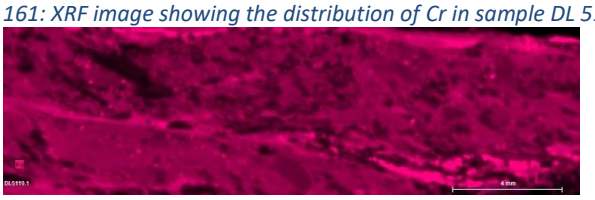

Figure 163: XRF image showing the distribution of Fe in sample DL 5119.1

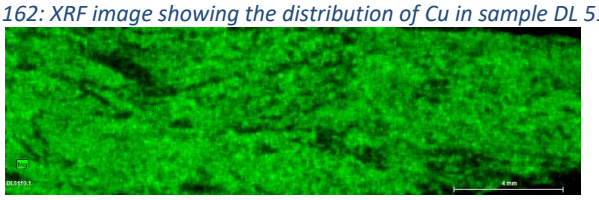

Figure 164: XRF image showing the distribution of Mg in sample DL 5119.1

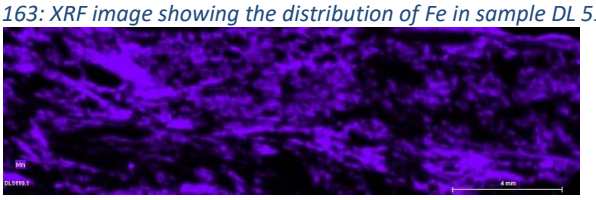

Figure 165: XRF image showing the distribution of Mn in sample DL 5119.1

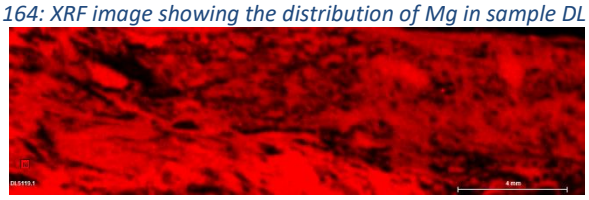

Figure 166: XRF image showing the distribution of Ni in sample DL 5119.1

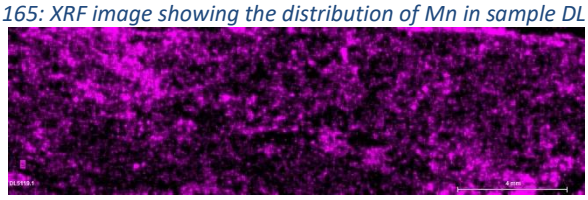

Figure 167: XRF image showing the distribution of S in sample DL 5119.1

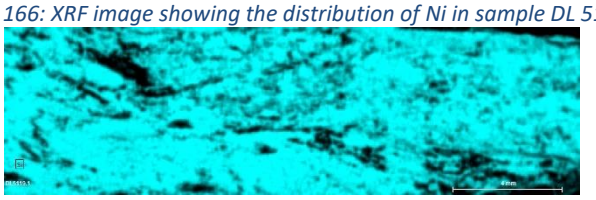

Figure 168: XRF image showing the distribution of Si in sample DL 5119.1

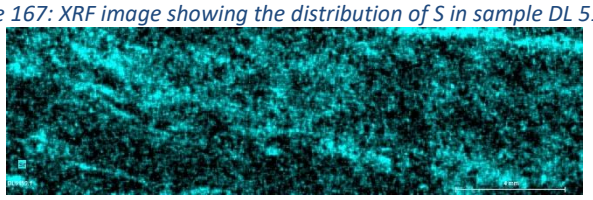

Figure 169: XRF image showing the distribution of Sr in sample DL 5119.1

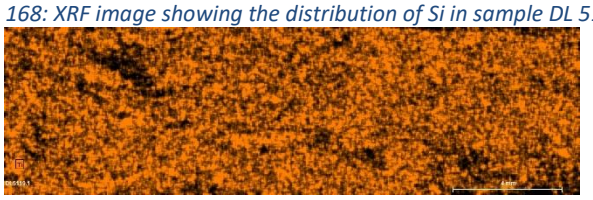

Figure 170: XRF image showing the distribution of Ti in sample DL 5119.1

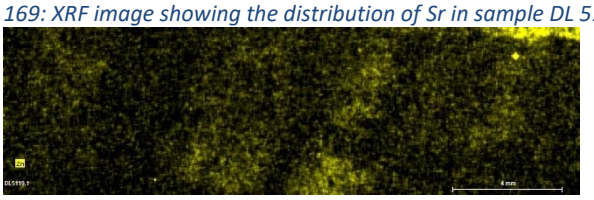

Figure 171: XRF image showing the distribution of Zn in sample DL 5119.1

Section ix: Sample DL 5119.2A

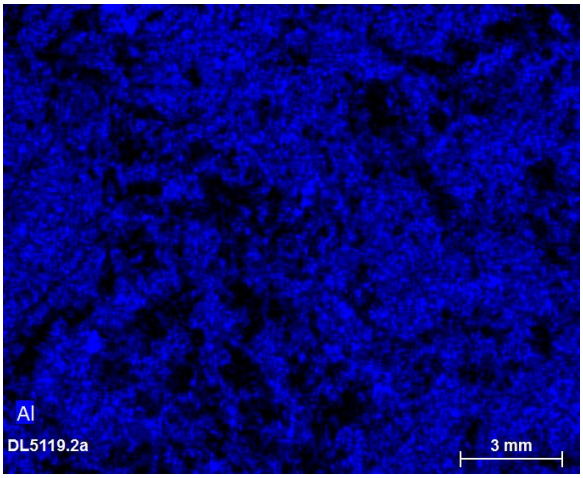

Figure 172: XRF image showing the distribution of Al in sample DL 5119.2A

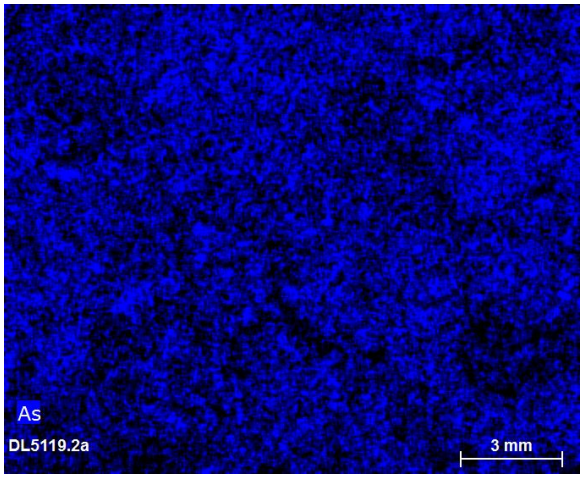

Figure 173: XRF image showing the distribution of As in sample DL 5119.2A

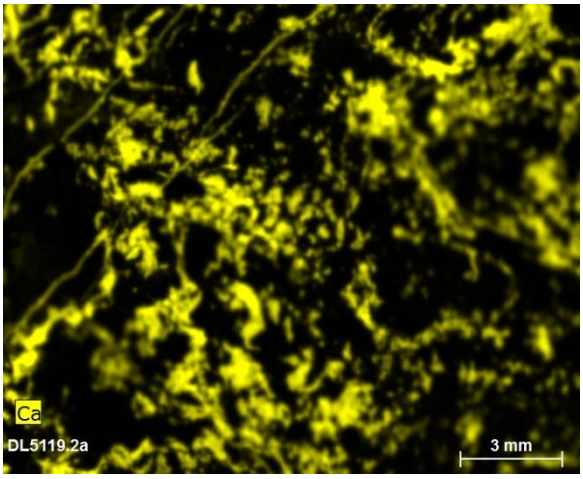

Figure 174: XRF image showing the distribution of Ca in sample DL 5119.2A

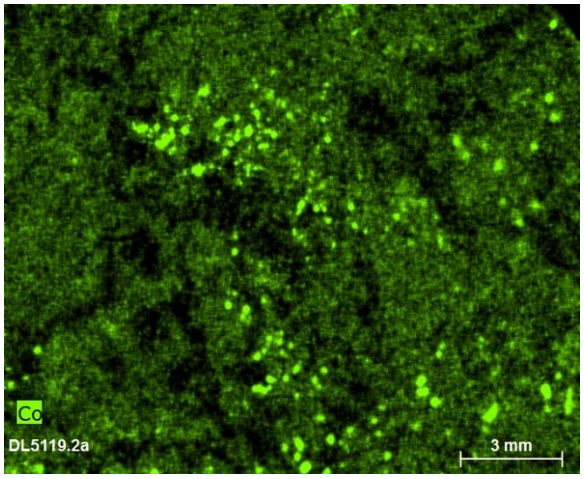

Figure 175: XRF image showing the distribution of Co in sample DL 5119.2A

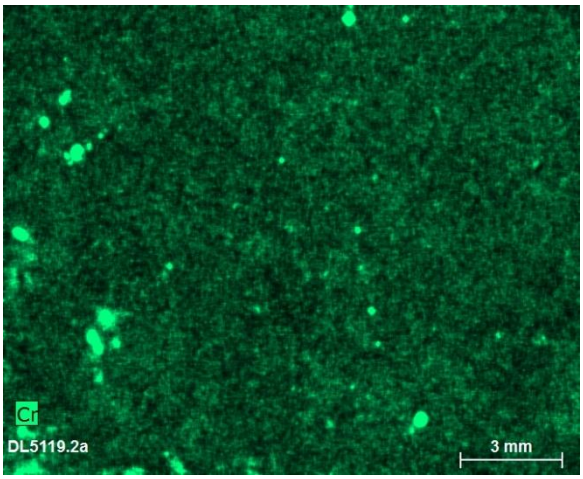

Figure 176: XRF image showing the distribution of Cr in sample DL 5119.2A

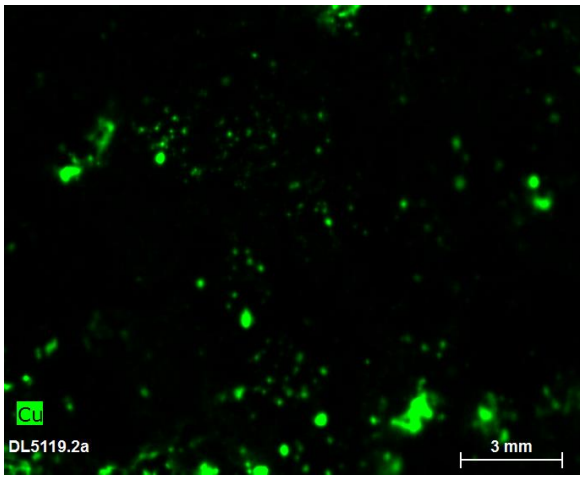

Figure 177: XRF image showing the distribution of Cu in sample DL 5119.2A

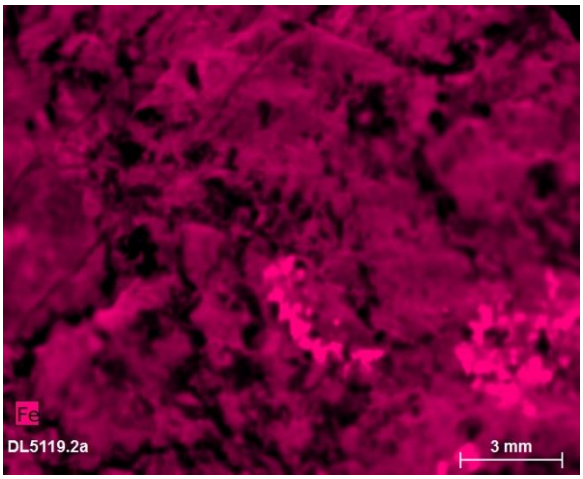

Figure 178: XRF image showing the distribution of Fe in sample DL 5119.2A

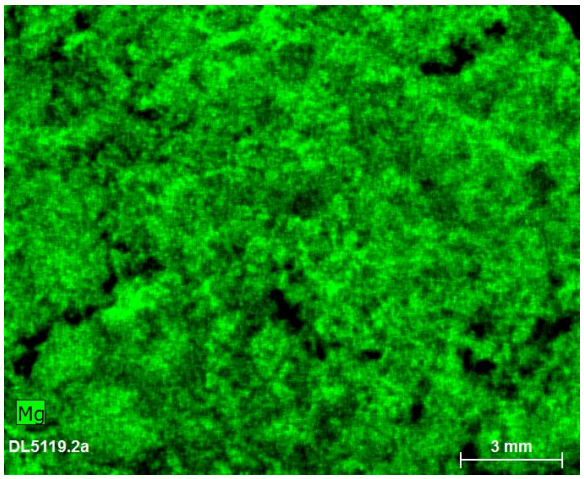

Figure 179: XRF image showing the distribution of Mg in sample DL 5119.2A

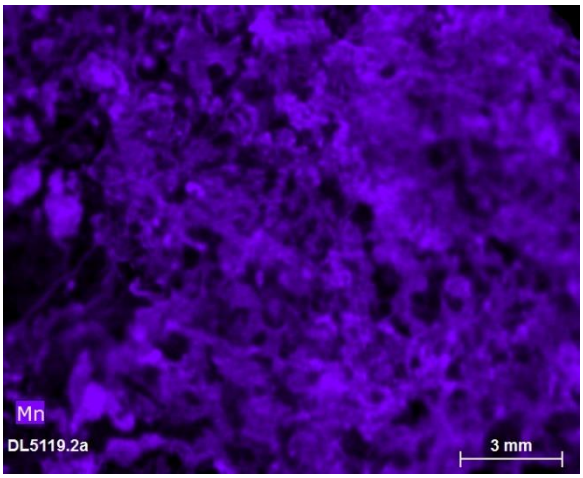

Figure 180: XRF image showing the distribution of Mn in sample DL 5119.2A

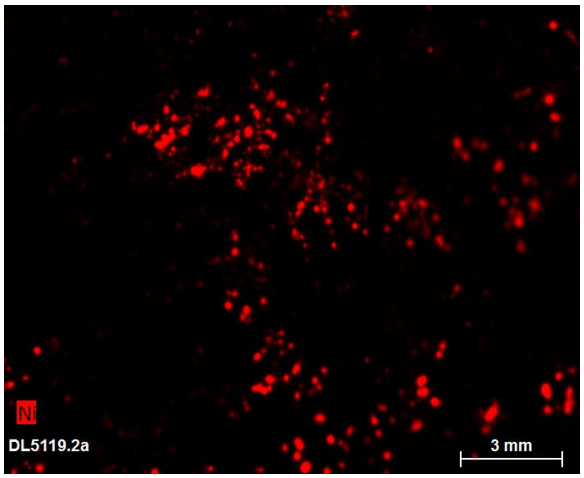

Figure181: XRF image showing the distribution of Ni in sample DL 5119.2A

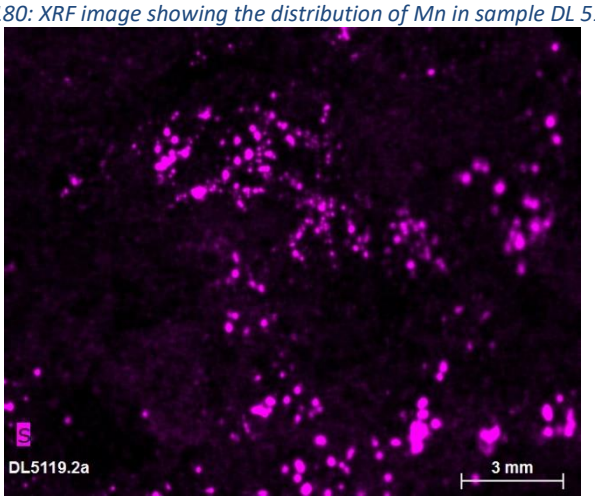

Figure 182: XRF image showing the distribution of S in sample DL 5119.2A

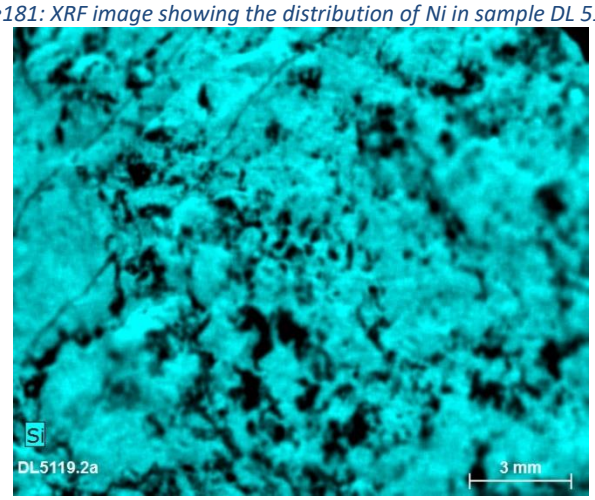

Figure 183: XRF image showing the distribution of Si in sample DL 5119.2A

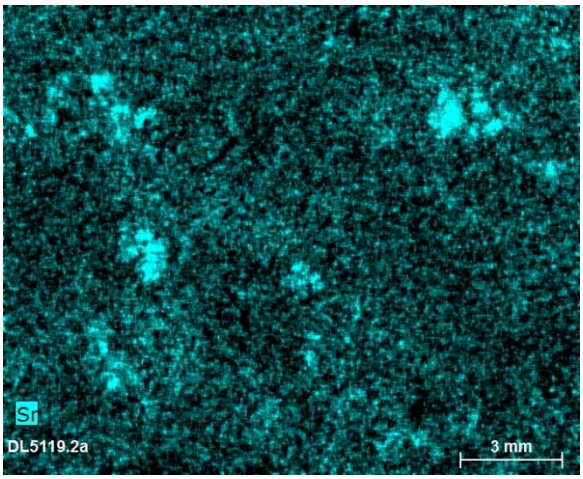

Figure 184: XRF image showing the distribution of Sr in sample DL 5119.2A

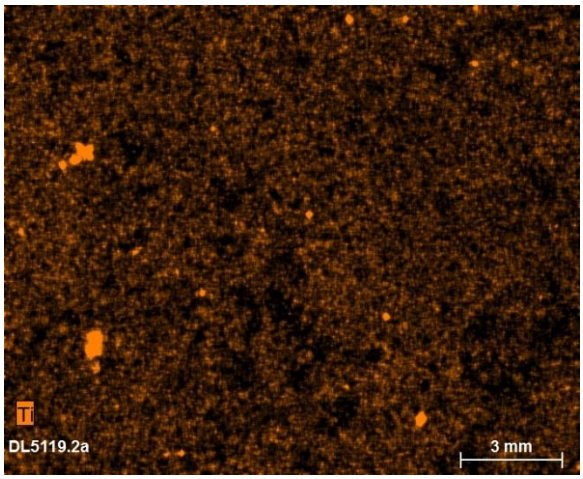

Figure 185: XRF image showing the distribution of Ti in sample DL 5119.2A

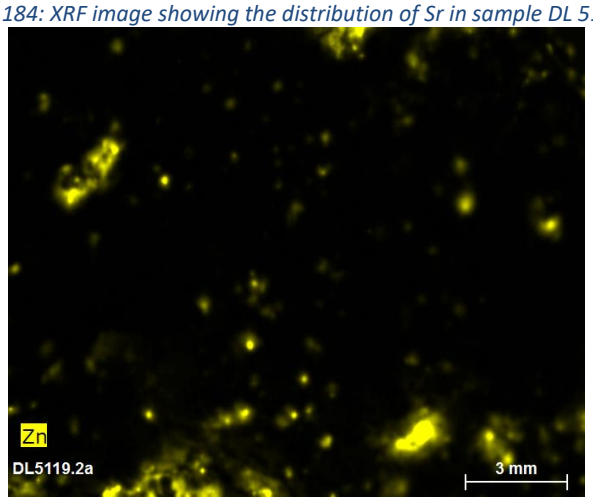

Figure 186: XRF image showing the distribution of Zn in sample DL 5119.2A